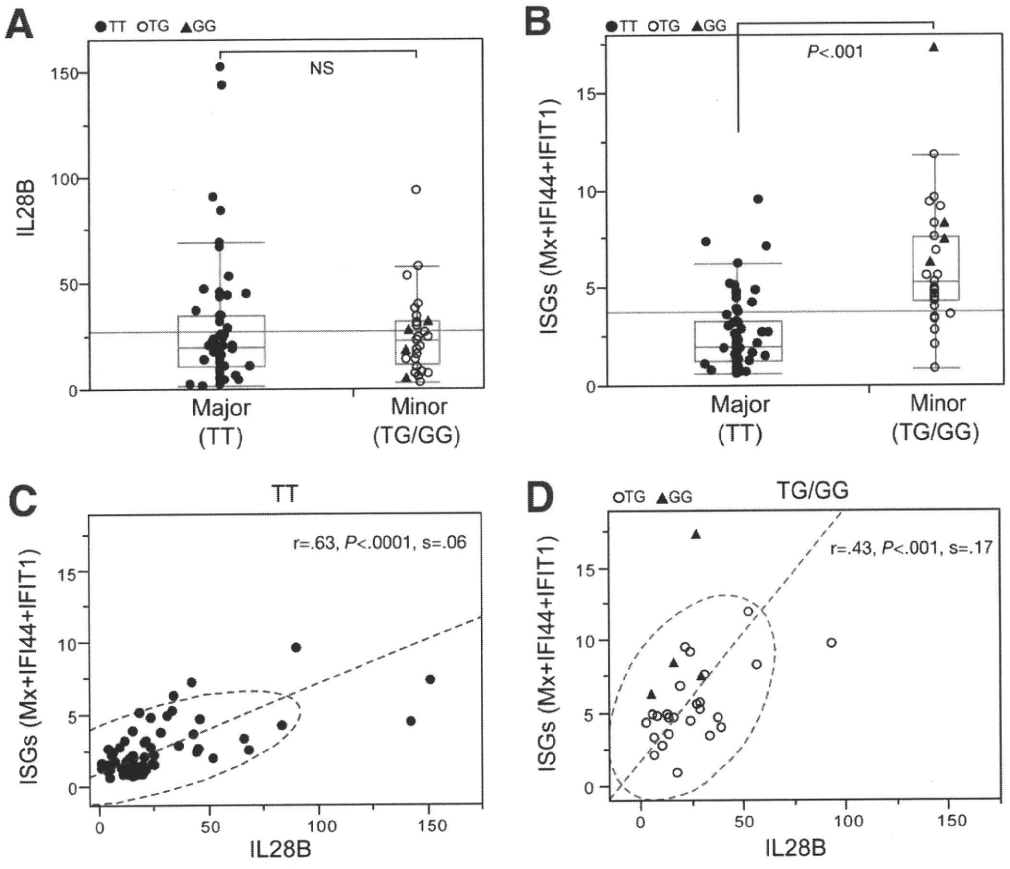

Figure 3. (*A*) IL28 expression in the liver of 91 patients with the major (TT) or minor (TG or GG) genotype (rs8099917). (*B*) Expression of ISGs in the liver of patients with the major (TT) or minor (TG or GG) genotype (rs8099917). (*C*) Relationship between IL28 and ISGs in the liver of patients with the major (TT) genotype (rs8099917). (*D*) Relationship between IL28 and ISGs in the liver of patients with the minor (TG or GG) genotype (rs8099917).

expression of IL28B may be a reason for the decreased ability to distinguish differences in its expression. Another possibility may be the specificity of the IL28B primers used in this study; because IL28B shares a 98.2% nucleotide sequence homology with IL28A, IL28B specific primers are not available.[21] When the expression of IL28B and hepatic ISGs were compared, a significant correlation was observed, and, interestingly, IL28B and ISGs derived from different SNPs were correlated in a different way (Figure 3*C* and *D*). It appeared that hepatic ISGs were more induced by the reduced amounts of IL28B in patients with the minor genotype. The mechanism behind these findings has yet to be determined; however, IL28B interacts with a heterodimeric class II cytokine receptor that consists of IL-10 receptor β (IL-10Rβ) and IL-28 receptor α (IL-28Rα).[18,19] It is possible that IL28B could mediate antiviral signaling through IL-10 signaling as well as STAT1 activation. The Th 2 dominant signaling of IL28B may modulate signaling pathways in livers with CH-C and contributes to the different expression of ISGs. Another possibility may be that the cell origin of hepatic ISGs is different. A recent study revealed cell-type specific ISG expression in macrophages and hepatocytes, which could be related to the IFN response.[22] As more of the B-cell-, dendritic cell-, and natural killer cell-related genes were up-regulated in the liver of patients with the major genotype, ISGs could be expressed by these cells, whereas they are expressed by hepatocytes in the liver of patients with the minor genotype. It is known that the induction of ISGs in lymphocytes is lower than that in hepatocytes. The precise mechanism should be investigated further as a different regulatory mechanism for the expression of ISGs may be present.

In conclusion, we presented the clinical relevance of the expression of hepatic ISGs for the treatment outcome of Peg-IFN and RBV combination therapy. The different expressions of hepatic ISGs before treatment might be due to polymorphisms in IL28B. Further studies are required to clarify the detailed pathways of IL28B and hepatic gene expression through molecular biologic and immunologic aspects.

Supplementary Material

Note: To access the supplementary material accompanying this article, visit the online version of *Gastroenterology* at www.gastrojournal.org, and at doi: 10.1053/j.gastro.2010.04.049.

Appendix 1. The Hokuriku Liver Study Group (HLSG) is Composed of the Following Members:

Drs Takashi Kagaya, Kuniaki Arai, Kaheita Kakinoki, Kazunori Kawaguchi, Hajime Takatori, Hajime Sunakosaka (Department of Gastroenterology, Kanazawa University Graduate School of Medicine, Kanazawa); Drs Touru

Nakahama, Shinji Kamiyamamoto (Kurobe City Hospital, Kurobe, Toyama); Dr Yasuhiro Takemori (Toyama Rosai Hospital, Uozu, Toyama); Dr Hikaru Oguri (Koseiren Namerikawa Hospital, Namerikawa, Toyama); Drs Yatsugi Noda, Hidero Ogino (Toyama Prefectural Central Hospital, Toyama, Toyama); Drs Yoshinobu Hinoue, Keiji Minouchi (Toyama City Hospital, Toyama, Toyama); Dr Nobuyuki Hirai (Koseiren Takaoka Hospital, Takaoka, Toyama); Drs Tatsuho Sugimoto, Koji Adachi (Tonami General Hospital, Tonami, Toyama); Dr Yuichi Nakamura (Noto General Hospital, Nanao, Ishikawa); Drs Masashi Unoura, Ryuhei Nishino (Public Hakui Hospital, Hakui, Ishikawa); Drs Hideo Morimoto, Hajime Ohta (National Hospital Organization Kanazawa Medical Center, Kanazawa, Ishikawa); Dr Hirokazu Tsuji (Kanazawa Municipal Hospital, Kanazawa, Ishikawa); Drs Akira Iwata, Shuichi Terasaki (Kanazawa Red Cross Hospital, Kanazawa, Ishikawa); Drs Tokio Wakabayashi, Yukihiro Shirota (Saiseikai Kanazawa Hospital, Kanazawa, Ishikawa); Drs Takeshi Urabe, Hiroshi Kawai (Public Central Hospital of Matto Ishikawa, Hakusan, Ishikawa); Dr Yasutsugu Mizuno (Nomi Municipal Hospital, Nomi, Ishikawa); Dr Shoni Kameda (Komatsu Municipal Hospital, Komatsu, Ishikawa); Drs Hirotoshi Miyamori, Uichiro Fuchizaki (Keiju Medical Center, Nanao, Ishikawa); Dr Haruhiko Shyugo (Kanazawa Arimatsu Hospital, Kanazawa, Ishikawa); Dr Hideki Osaka (Yawata Medical Center, Komatsu, Ishikawa); Dr Eiki Matsushita (Kahoku Central Hospital, Tsubata, Ishikawa); Dr Yasuhiro Katou (Katou Hospital, Komatsu, Ishikawa); Drs Nobuyoshi Tanaka, Kazuo Notsumata (Fukuiken Saiseikai Hospital, Fukuil, Fukui); Dr Mikio Kumagai (Kumagai Clinic, Tsuruga, Fukui); Dr Manabu Yoneshima (Municipal Tsuruga Hospital, Tsuruga, Fukui).

References

1. Kiyosawa K, Sodeyama T, Tanaka E, et al. Interrelationship of blood transfusion, non-A, non-B hepatitis and hepatocellular carcinoma: analysis by detection of antibody to hepatitis C virus. Hepatology 1990;12:671–675.
2. Fried MW, Shiffman ML, Reddy KR, et al. Peginterferon alfa-2a plus ribavirin for chronic hepatitis C virus infection. N Engl J Med 2002;347:975–982.
3. Poynard T, Ratziu V, McHutchison J, et al. Effect of treatment with peginterferon or interferon alfa-2b and ribavirin on steatosis in patients infected with hepatitis C. Hepatology 2003;38:75–85.
4. Enomoto N, Sakuma I, Asahina Y, et al. Mutations in the nonstructural protein 5A gene and response to interferon in patients with chronic hepatitis C virus 1b infection. N Engl J Med 1996; 334:77–81.
5. Okanoue T, Itoh Y, Hashimoto H, et al. Predictive values of amino acid sequences of the core and NS5A regions in antiviral therapy for hepatitis C: a Japanese multi-center study. J Gastroenterol 2009;44:952–963.
6. Feld JJ, Nanda S, Huang Y, et al. Hepatic gene expression during treatment with peginterferon and ribavirin: identifying molecular pathways for treatment response. Hepatology 2007;46:1548–1563.
7. Sarasin-Filipowicz M, Oakeley EJ, Duong FH, et al. Interferon signaling and treatment outcome in chronic hepatitis C. Proc Natl Acad Sci U S A 2008;105:7034–7039.
8. Asselah T, Bieche I, Narguet S, et al. Liver gene expression signature to predict response to pegylated interferon plus ribavirin combination therapy in patients with chronic hepatitis C. Gut 2008;57:516–524.
9. Chen L, Borozan I, Feld J, et al. Hepatic gene expression discriminates responders and nonresponders in treatment of chronic hepatitis C viral infection. Gastroenterology 2005;128:1437–1444.
10. Thomas DL, Thio CL, Martin MP, et al. Genetic variation in IL28B and spontaneous clearance of hepatitis C virus. Nature 2009; 461:798–801.
11. Ge D, Fellay J, Thompson AJ, et al. Genetic variation in IL28B predicts hepatitis C treatment-induced viral clearance. Nature 2009;461:399–401.
12. Tanaka Y, Nishida N, Sugiyama M, et al. Genome-wide association of IL28B with response to pegylated interferon-α and ribavirin therapy for chronic hepatitis C. Nat Genet 2009;41:1105–1109.
13. Desmet VJ, Gerber M, Hoofnagle JH, et al. Classification of chronic hepatitis: diagnosis, grading and staging. Hepatology 1994;19:1513–1520.
14. Honda M, Yamashita T, Ueda T, et al. Different signaling pathways in the livers of patients with chronic hepatitis B or chronic hepatitis C. Hepatology 2006;44:1122–1138.
15. Honda M, Kaneko S, Kawai H, et al. Differential gene expression between chronic hepatitis B and C hepatic lesion. Gastroenterology 2001;120:955–966.
16. Shipley B. A new inferential test for path models based on directed acyclic graphs. Structural Equation Modeling 2000;7:206–218.
17. Favre M, Martin J, Festa-Bianchet M. Determinants and life-history consequences of social dominance in bighorn ewes. Anim Behav 2008;76:1373–1380.
18. Sheppard P, Kindsvogel W, Xu W, et al. IL-28, IL-29, and their class II cytokine receptor IL-28R. Nat Immunol 2003;4:63–68.
19. Kotenko SV, Gallagher G, Baurin VV, et al. IFN-λ mediate antiviral protection through a distinct class II cytokine receptor complex. Nat Immunol 2003;4:69–77.
20. Camma C, Bruno S, Di Marco V, et al. Insulin resistance is associated with steatosis in nondiabetic patients with genotype 1 chronic hepatitis C. Hepatology 2006;43:64–71.
21. Mihm S, Frese M, Meier V, et al. Interferon type I gene expression in chronic hepatitis C. Lab Invest 2004;84:1148–1159.
22. Chen L, Borozan I, Sun J, et al. Cell-type specific gene expression signature in liver underlies response to interferon therapy in chronic hepatitis C infection. Gastroenterology 2010;138:942–948.

Received October 9, 2009. Accepted April 14, 2010.

Reprint requests

Address requests for reprints to: Shuchi kaneko, MD, PhD, Department of Gastroenterology, Graduate School of Medicine, Kanazawa University, Takara-Machi 13-1, Kanazawa 920-8641, Japan. e-mail: skaneko@m-kanazawa.jp; fax: (81) 76-234-4250.

Acknowledgments

The authors thank Nami Nishiyama and Yuki Hatayama for excellent technical assistance.

Participating investigators are listed in Appendix 1.

Conflicts of interest

The authors disclose no conflicts.

Funding

This work was supported in part by a grant-in-aid from the Ministry of Health, Labour and Welfare of Japan.

Altered Hepatic Gene Expression Profiles Associated With Myocardial Ischemia

Hiroshi Ootsuji, MD; Masao Honda, MD, PhD; Shuichi Kaneko, MD, PhD; Soichiro Usui, MD, PhD; Masaki Okajima, MD, PhD; Hikari Okada, MS; Yoshio Sakai, MD, PhD; Toshinari Takamura, MD, PhD; Katsuhisa Horimoto, PhD; Masayuki Takamura, MD, PhD

Background—Acute coronary syndrome is sometimes accompanied by accelerated coagulability, lipid metabolism, and inflammatory responses, which are not attributable to the cardiac events alone. We hypothesized that the liver plays a pivotal role in the pathophysiology of acute coronary syndrome. We simultaneously analyzed the gene expression profiles of the liver and heart during acute myocardial ischemia in mice.

Methods and Results—Mice were divided into 3 treatment groups: sham operation, ischemia/reperfusion, and myocardial infarction. Mice with liver ischemia/reperfusion were included as additional controls. Marked changes in hepatic gene expression were observed after 24 hours, despite the lack of histological changes in the liver. Genes related to tissue remodeling, adhesion molecules, and morphogenesis were significantly upregulated in the livers of mice with myocardial ischemia/reperfusion or infarction but not in those with liver ischemia/reperfusion. Myocardial ischemia, but not changes in the hemodynamic state, was postulated to significantly alter hepatic gene expression. Moreover, detailed analysis of the signaling pathway suggested the presence of humoral factors that intervened between the heart and liver. To address these points, we used isolated primary hepatocytes and showed that osteopontin released from the heart actually altered the signaling pathways of primary hepatocytes to those observed in the livers of mice under myocardial ischemia. Moreover, osteopontin stimulated primary hepatocytes to secrete vascular endothelial growth factor-A, which is important for tissue remodeling.

Conclusions—Hepatic gene expression is potentially regulated by cardiac humoral factors under myocardial ischemia. These results provide new insights into the pathophysiology of acute coronary syndrome. (***Circ Cardiovasc Genet.* 2010;3:68-77.**)

Key Words: coronary disease ■ genetics ■ liver ■ myocardial infarction

In addition to chest pain, acute coronary syndrome (ACS) is sometimes accompanied by systemic manifestations, such as proinflammatory responses, activation of the coagulation-fibrinolytic system, and lipid metabolism.[1–3] These are considered to be systemic reactions involving multiple organs, which exacerbate the cardiac events.

Clinical Perspective on p 77

C-reactive protein, coagulation factors, and protein C, the levels of which fluctuate in ACS, are liver-specific factors. Although these reports were based on a limited number of factors, the observations suggest a close relation between the liver and myocardial ischemia and imply that the liver plays a pivotal role in the pathophysiology of ACS.

cDNA microarray technology allows simultaneous analysis of the expression levels of thousands of genes. Genome-based expression profiling provides useful information on the molecular pathogenesis of various diseases as well as disease progression and prognosis.[4–7] Previous microarray studies have examined the molecular dynamics of the myocardium induced by myocardial ischemia.[8,9] However, global gene expression analyses applied to the liver affected by myocardial ischemia have not been reported.

In this study, we examined the responses of hepatic gene expression to myocardial ischemia. Given the systemic inflammation that characterizes ACSs, we postulated that regulation of hepatic genes occurs by inflammatory mediators and not by alterations in hemodynamics or hepatic perfusion. Therefore, we used whole-genome transcriptional profiling to identify hepatic genes selectively regulated in myocardial ischemia.

Methods

This study was approved by institutional and governmental animal research committees and was conducted in accordance with the *Guide for the Care and Use of Laboratory Animals* published by the US National Institutes of Health (NIH publication No. 85-23, revised 1996). C57BL/6J mice (n=46; body weight, 24.1±1.4 g; 8 to 10

Received June 1, 2008; accepted November 10, 2009.

From the Department of Disease Control and Homeostasis (H. Ootsuji, M.H., S.K., S.U., M.O., H. Okada, Y.S., T.T., M.T.), Kanazawa University Graduate School of Medical Science, Kanazawa University, Kanazawa, Japan; and National Institute of Advanced Industrial Science and Technology (K.H.), Tokyo, Japan.

The online-only Data Supplement is available at http://circgenetics.ahajournals.org/cgi/content/full/CIRCGENETICS.108.795484.

Correspondence to Shuichi Kaneko, MD, PhD, Department of Disease Control and Homeostasis, Kanazawa University Graduate School of Medical Science, Kanazawa University, 13-1 Takara-machi, Kanazawa 920-8641, Japan. E-mail skaneko@m-kanazawa.jp

Circ Cardiovasc Genet **is available at http://circgenetics.ahajournals.org** **DOI: 10.1161/CIRCGENETICS.108.795484**

Table 1. Biochemical Assessment

		6 h				24 h			
	Before Operation	Sham	I/R	Infarction	Liver I/R	Sham	I/R	Infarction	Liver I/R
No.	5	5	5	5	5	6	5	5	5
CPK, U/L	944±98	5031±646	11597±1272*	19830±1154*	8673±1379	1702±181	1913±184	2939±515†	1595±349
AST, U/L	94±4	674±41	899±21*	1858±59*	414±43	200±19	277±14	661±28*	163±22
ALT, U/L	58±4	119±9	115±6	153±7	143±18	46±3	64±6	107±11*	42±3
LDH, U/L	652±32	2684±206	3432±80†	5264±111*	2478±446	681±72	867±37	2095±164*	862±209

Values are presented as mean±SE. CPK indicates creatine kinase; AST, aspartate aminotransferase; ALT, alanine aminotransferase; and LDH, lactate dehydrogenase.

*$P<0.01$ compared with sham.

†$P<0.05$ compared with sham.

weeks of age; Charles River Laboratories, Yokohama, Japan) were divided into the following treatment groups: sham operation (n=11), ischemia/reperfusion (I/R; n=10), myocardial infarction (MI; n=10), liver I/R (n=10), and sham operation plus hydralazine (n=5). Hepatic gene expression was evaluated among these groups, and the results were further investigated in primary mouse hepatocytes.

Additional Methods

An expanded Methods section containing details of animal surgery, hydralazine group, liver I/R group, blood sampling and analysis, histopathological analysis, blood pressure and heart rate measurements, microarray experiments, processing of cDNA microarray data, extraction of significantly upregulated cardiac and hepatic genes, pathway analysis, ELISA for secreted osteopontin and vascular endothelial growth factor (*VEGF*), primary hepatocyte experiments, and quantitative real-time detection polymerase chain reaction (RTD-PCR) is available in the online-only Data Supplement.

All microarray data have been deposited in the National Center for Biotechnology Information Gene Expression Omnibus database with the series accession number GSE14843.

Data Analysis

The data are presented as the mean±SEM for each group of mice and were analyzed by ANOVA with Bonferroni post hoc test for multiple comparisons. Statistical analyses of blood sampling, blood pressure, and heart rate were performed with the Steel (heterogeneity of variance) multicomparison test. Significance was set at $P<0.05$. Statistical analyses were performed with SAS statistical software (SAS Institute Japan, Tokyo, Japan).

Results

Establishment of Cardiac I/R or MI in Mice

Cardiac I/R or MI was successfully induced in normal C57BL/6J mice. The levels of cardiac enzymes, such as creatine kinase, aspartate aminotransferase, and lactate dehydrogenase, increased significantly after 6 hours in the I/R group and showed markedly greater increases in the infarction group compared with the sham group (Table 1). In addition, the normalization of these enzyme levels was reduced after 24 hours in the infarction group.

Histologically, azan or hematoxylin/eosin staining showed wall thinning, coagulation necrosis, and transmural fibrosis in the risk area in the infarction group but not in the I/R group (data not shown). As shown in Table 2, no significant differences were found in heart rate or blood pressure after 24 hours compared with the preoperative values in the sham and I/R groups, whereas a decrease in blood pressure was found in the infarction group.

Histological Assessment of the Liver After Cardiac I/R or MI

The I/R and infarction groups showed a minimal, but transient, increase in alanine aminotransferase ALT. Although alanine aminotransferase may be released from the myocardium[10] rather than from the liver, to exclude the effect of the transient change in hepatic venous pressure associated with cardiogenic shock, we examined histological changes in the liver after myocardial I/R or infarction. No histological abnormalities were observed in the shocked liver, as indicated by the lack of hepatocyte necrosis in acinar zone 3 in the sham, I/R, and infarction groups (Figure 1a, 1c, 1e, and 1g; hematoxylin/eosin staining). In addition, no signs of liver congestion were observed, as indicated by the lack of dilatation of the terminal hepatic venules and adjacent sinusoids in the sham, I/R, or infarction group (Figure 1b, 1d, 1f, and 1h; silver staining).

On transmission electron microscopy, no ischemic changes, such as swelling or loss of cristae in the mitochondria, a mixed irregular pattern or swelling of the rough endoplasmic reticulum, or dilatation or indistinct appearance of the sinusoids, were observed in the sham, I/R, or infarction group (Figure 2A through 2C). Based on these results, histological analysis did not demonstrate the presence of shock or congestive liver in the I/R or infarction group.

Changes in the Hepatic Gene Expression Profile After Cardiac I/R or MI

Although no histological changes were observed in the liver after cardiac I/R or MI, significant changes in gene expression were noted. Hierarchical clustering analysis, which is a nonsupervised learning method that includes 23 281 nonfil-

Table 2. HR, sBP, and mBP

		24 h		
	Before Operation	Sham	I/R	Infarction
HR, bpm	575±27	553±30	553±27	568±16
sBP, mm Hg	105±2	102±2	95±1	80±4*
mBP, mm Hg	78±3	74±2	63±2	56±4†

Values are presented as mean±SE. HR indicates heart rate; sBP, systolic blood pressure; and mBP, mean blood pressure.

*$P<0.01$ compared with sham.

†$P<0.05$ compared with sham.

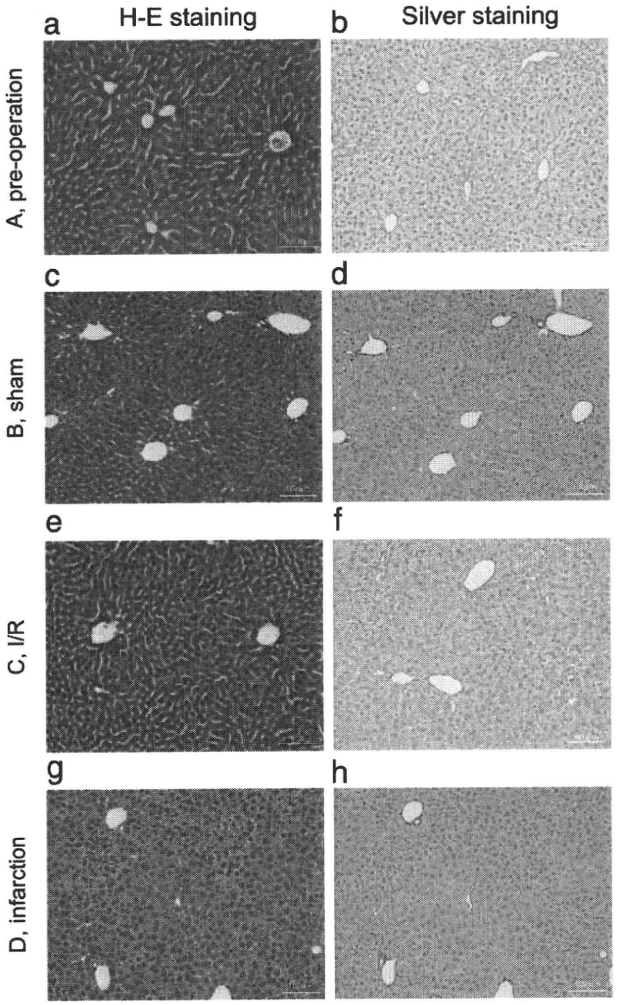

Figure 1. Histological comparison of hematoxylin/eosin staining and silver staining of the liver after 24 hours. Preoperation (A), sham (B), I/R (C), and infarction (D). Scale bars represent 100 μm. Hematoxylin/eosin staining (a, c, e, and g); silver staining (b, d, f, and h). No indication of shock or congestive liver was observed in any group (magnification, ×200).

tered genes, produced clusters for the I/R or infarction group and the sham-operated group (data not shown). Because nonfiltered genes may include those that are unchanged in all samples, which generated "noise" that prevented efficient gene clustering, we filtered out these genes with different stringency and performed hierarchical clustering. Hierarchical clustering with 9165 (log-ratio variations >40th percentile) or 5156 (log-ratio variations >50th percentile) filtered genes clearly demonstrated clusters for the I/R or infarction group after 24 hours, for the I/R or infarction group after 6 hours, and for the sham group after 6 and 24 hours (supplemental Figure I). Hierarchical clustering with 773 (log-ratio variations >80th percentile) or 96 (log-ratio variations >90th percentile) filtered genes showed more detailed and clearer clusters for the I/R group after 24 hours, for the infarction group after 24 hours, for the I/R or infarction group after 6 hours, and for the sham group after 6 and 24 hours (Figure 3). Thus, by filtering out "noise" genes, more detailed and clearer clustering could be obtained, thus addressing the reliability of the analysis.[11] The increased robustness (R-

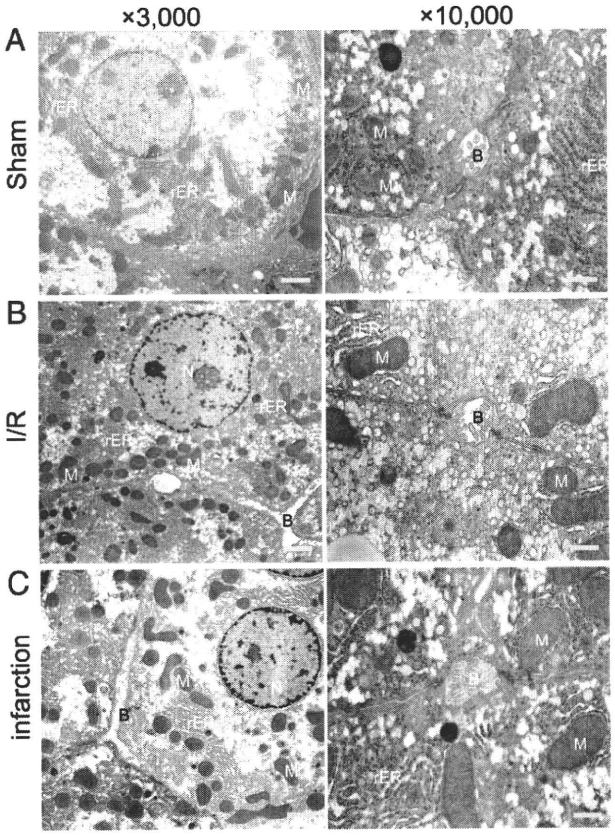

Figure 2. Representative electron microphotographs of the liver after 24 hours. Sham (A), I/R (B), and infarction (C). Scale bars represent 2 μm on the left (magnification, ×3000) and 500 nm on the right (magnification, ×10 000). No indication of shocked liver was observed in any group. M indicates mitochondria; rER, rough endoplasmic reticulum; B, bile canaliculi; N, nucleus.

index) and decreased discrepancy (D-index) of clustering with filtering conditions supported this finding (supplemental Figure I; expanded Methods and Results).

Class prediction analysis, a supervised learning method based on the compound covariate predictor, was performed with various clinical parameters, including provocation (I/R or infarction), 6 hours (I/R or infarction after 6 hours), 24 hours (I/R or infarction after 24 hours), and time (sham or 6 hours, sham or 24 hours, and 6 or 24 hours). The results

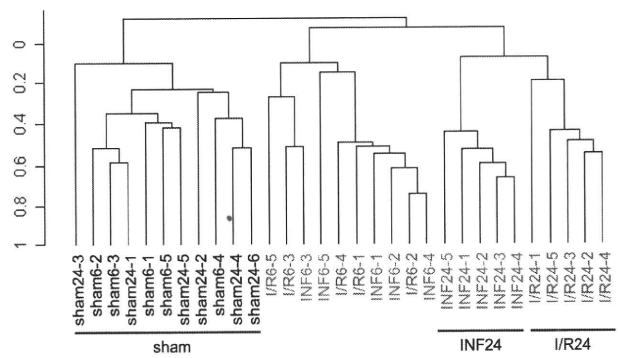

Figure 3. Hierarchical clustering analysis with 96 filtered genes (genes with log-ratio variation in the 90th percentile and data missing >5% were excluded). The resulting dendrogram shows clear clusters for the I/R group after 24 hours, the infarction group after 24 hours, and the sham group after 6 and 24 hours.

Table 3. Class Prediction Analysis (Supervised Learning Methods)

Classifier Category	Clinical Group	Total No. of Classes	No. of Cases Misclassified	Classifier *P*	Mean Percent of Correct Classification	No. of Genes in the Classifiers ($P<0.002$)
Provocation	I/R	10	2	0.02	80	85
	INF	10	2			
6 h	I/R	5	2	0.48	50	23
	INF	5	3			
24 h	I/R	5	0	0.015	100	218
	INF	5	0			
Time	Sham	11	0	0.001	90	644
	6 h	10	2			
	Sham	11	0	<0.0005	95	3380
	24 h	10	1			
	6 h	10	1	0.004	85	747
	24 h	10	2			

INF indicates infarction.

indicated that provocation, 24 hours, and time significantly classified these models (Table 3).

Both nonsupervised and supervised learning methods indicated differences in hepatic gene expression profiling among sham, 6 hours, and 24 hours after heart provocation, and different heart provocation (I/R or infarction) may generate differences in hepatic gene expression, especially 24 hours after provocation.

Identification of Genes Differentially Expressed Between I/R and Infarction

Because the filtering process may result in loss of important genes, for identification of differentially expressed genes among different groups, we used a class comparison analysis tool (http://linus.nci.nih.gov/BRB-ArrayTools.html). Class comparison analysis ($P<0.0005$) among the 5 groups (ie, sham, I/R-6, I/R-24, infarction-6, and infarction-24) was performed, and genes that were differentially expressed among the 5 groups were extracted. On 1-way hierarchical clustering analysis of the extracted genes and heat map, 6 gene clusters were assigned on the basis of the gene expression patterns (Figure 4). Of the 6 groups, group 2 showed significant upregulation for I/R and infarction after 24 hours compared with the other groups. Group 3 showed upregulation for I/R, but not for infarction, after 24 hours. Group 4 showed downregulation for I/R and infarction after 24 hours compared with the other groups. Group 5 showed downregulation for infarction after 24 hours compared with the other groups. Representative genes (>3-fold difference in *t* value) and frequent pathways observed in each group (based on the MetaCore database) are listed in supplemental Tables I through IV.

Interestingly, in group 2, genes related to tissue remodeling, adhesion molecules, and morphogenesis were significantly upregulated. This may be related to the induction of tissue repair factors, such as antigenic factor and myocardiogenic factors, associated with I/R or infarction. In addition, genes involved in the cell cycle and apoptosis and neuron-related genes, such as retinoblastoma 1, angiopoietin-like 4, apoptotic peptidase-activating factor 1, transformation-related protein 53 (*p53*), and Eph receptor B1, were preferentially expressed. The expression of group 2 genes was significantly correlated with serum creatine kinase levels, suggesting that these genes reflect the severity of cardiac damage. Especially, ($R=0.856$, $P<e^{-07}$) and apoptotic peptidase-activating factor 1 ($R=0.856$, $P<e^{-07}$) were highly correlated with creatine kinase (supplemental Table I).

In group 3, in addition to the genes described earlier, chemokine and hormone gene pathways involved in interleukin (IL)-8 and androgen or estrogen receptor signaling were upregulated, suggesting that more tissue repair and bioreactive signaling pathways were activated. This may reflect the presence of a living myocyte I/R condition. In group 4, genes involved in lipid catabolism, immune response, proteolysis, and oxidative stress, such as apolipoprotein A-II, CD7 antigen, and reduced nicotinamide-adenine dinucleotide phosphate oxidase 1, were downregulated in the infarction and I/R groups after 24 hours. In group 5, genes involved in muscle and neurite morphogenesis, such as myosin (heavy polypeptide 11, smooth muscle) and ephrin A5, were significantly downregulated in the infarction group after 24 hours.

Effects of Hemodynamic State on Hepatic Gene Expression Profile

To exclude the possibility that changes in hemodynamic state induced alterations in hepatic gene expression, we examined the livers of mice subjected to liver I/R. For liver I/R, gentle occlusion of the hepatic artery and portal vein was applied so that the extent of liver injury was comparable with those in the myocardial I/R and infarction models (Table 1).

We analyzed the gene expression profile of the liver I/R group by using the same extracted genes as shown in Figure 4. The gene expression patterns induced in the myocardial I/R and infarction groups are clearly different from those in the liver I/R group (Figure 5), except for the group 3 gene cluster in myocardial I/R. It should be noted that the group 3 gene cluster was upregulated in the myocardial I/R group at 24

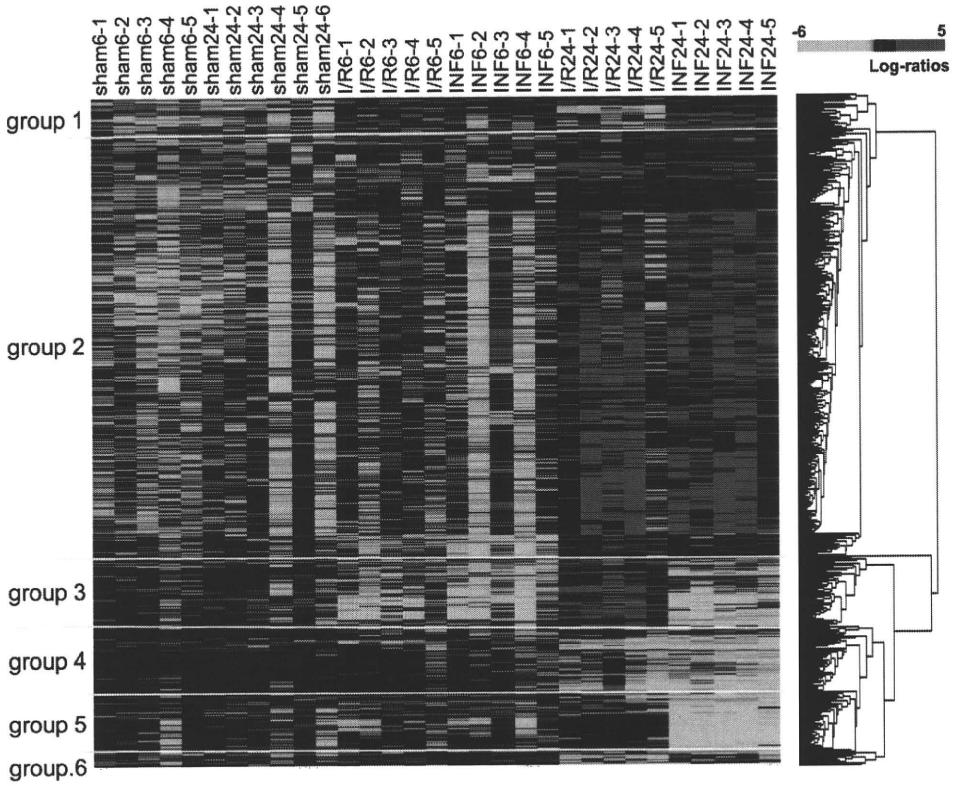

Figure 4. One-way hierarchical clustering and a heat map of 1166 genes that were extracted by class comparison analysis ($P<0.0005$). Each column corresponds to a sample, and each row represents a gene. The gene cluster data are graphically presented as colored images: red indicates upregulated genes, and green indicates downregulated genes. The genes with the most similar patterns of expression are adjacent to one another. Detailed definitions of each group are given in the text. Representative genes and frequently observed pathways are listed in supplemental Tables I through IV.

hours after provocation, whereas it was upregulated from 6 hours after provocation in the liver I/R group. Therefore, the delayed changes in hepatic gene expression in the myocardial I/R and infarction models may be due to different mechanisms resulting from liver I/R.

The assessment of liver weight revealed no differences between the myocardial I/R and infarction groups (supplemental Table V). This result supports our histological findings and indicates an absence of liver congestion in the myocardial I/R and infarction groups.

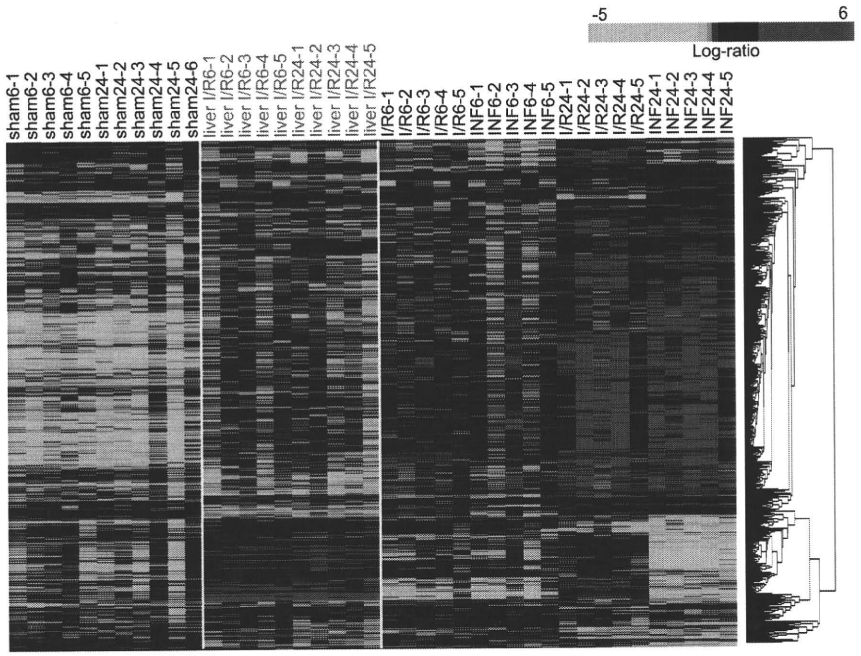

Figure 5. One-way hierarchical clustering and a heat map of the liver I/R group and others with the same extracted genes as shown in Figure 4. Each column corresponds to a sample, and each row represents a gene. The gene cluster data are graphically presented as colored images: red indicates upregulated genes, and green indicates downregulated genes. The genes with the most similar patterns of expression are adjacent to one another. Gene expression patterns induced in the liver I/R group clearly differed from those in the myocardial I/R and infarction groups.

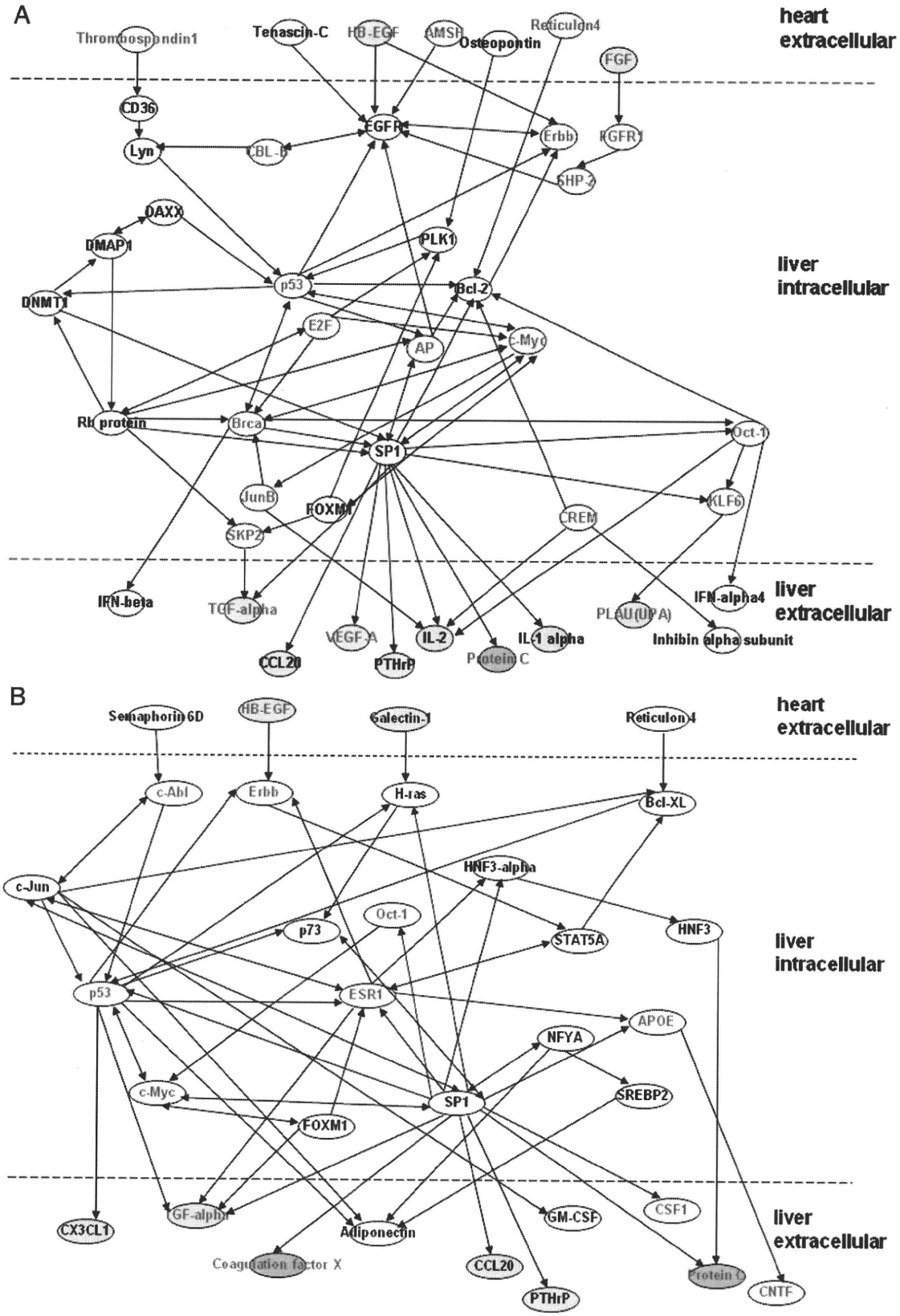

Figure 6. A, Postulated gene network of differentially expressed genes in infarction. B, Postulated gene network of differentially expressed genes in I/R. Detailed definitions of heart-extracellular, liver-intracellular, and liver-extracellular are given in the Methods. Yellow ovals indicate genes related to angiogenesis; green ovals, genes related to coagulation-fibrinolysis; blue ovals, genes related to inflammation; and red characters, genes upregulated in microarray analysis of primary hepatocytes treated with osteopontin. The network diagrams consist of representative genes. All abbreviations are defined in supplemental Tables VI through XI.

Detailed Gene Network Analysis Between the Liver and Heart in Myocardial Ischemia

Several factors can affect the liver, including humoral factors released from the ischemic myocardium, the hemodynamic state, or the autonomic nervous system. We focused on the possibility that humoral factors released from the heart may affect the liver. Cardiac gene expression profiles induced by myocardial ischemia were investigated to identify cardiac genes affecting the liver. To obtain a detailed and comprehensive gene network for the liver and heart, individual data from the liver after 24 hours were integrated with pooled data from the risk area and nonrisk area of the heart. Initially, we divided the heart and liver genes into 3 groups: heart-extracellular, liver-intracellular, and liver-extracellular. To find the network among these induced genes, published results for the interactions of individual genes were integrated with these results by using MetaCore software (GeneGo, St. Joseph, Mich). Direct interactions between individual genes were sought. Genes were excluded according to the following criteria: (1) heart-extracellular, no output signal into liver-intracellular; (2) liver-intracellular, no bidirectional signals; and (3) liver-extracellular, no input signal from liver-intracellular. As expected, the network of these differentially expressed genes involved complex interactions of individual genes; however, representative signaling pathways for MI or I/R injury were identified (Figure 6).

During MI, fibroblast growth factor, osteopontin, and heparin-binding epidermal growth factor-like growth factor (*HB-EGF*) were upregulated in the heart and may have been systemically secreted. Endothelial growth factor receptor and fibroblast growth factor receptor-1 may play important roles in receiving these signals in the liver. Transcription factors such as *p53*, myelocytomatosis oncogene, *trans*-acting transcription factor 1, and octamer-binding transcription factor 1 are important molecules in the regulation of these signaling pathways. Protein C, VEGF-A, and urokinase were expected to be systemically secreted from the liver (supplemental Tables VI through VIII). After infarction, genes involved in inflammation, the coagulation-fibrinolytic system, and angiogenesis showed preferential expression. After I/R, heparin-binding epidermal growth factor was upregulated in the heart and was expected to be systemically secreted. V-*erb*-a erythroblastic leukemia viral oncogene homolog 4 (avian) may play an important role in receiving these signals in the liver. Transcription factors such as *trans*-acting transcription factor 1, *p53*, estrogen receptor-1α, and signal transducer and activator of transcription 5A are potentially important molecules for regulation of these signaling pathways. Protein C, coagulation factor X, ciliary neurotrophic factor, and colony-stimulating factor-1 (macrophage) (*CSF-1*) were expected to be systemically secreted from the liver. In I/R, angiogenesis-related genes were preferentially upregulated (supplemental Tables IX through XI). On comparison of the expression profiles of the heart and liver, genes expressed at significantly higher levels in the heart than in the liver were designated as He, and those expressed at significantly higher levels in the liver than in the heart were designated as Li. Genes expressed in both the heart and liver were described as He/Li (supplemental Tables VIII and XI). In this analysis, most of the factors that were expected to be secreted from the liver induced by I/R and infarction were liver-specific. Most of these genes were not significantly upregulated in the liver I/R groups.

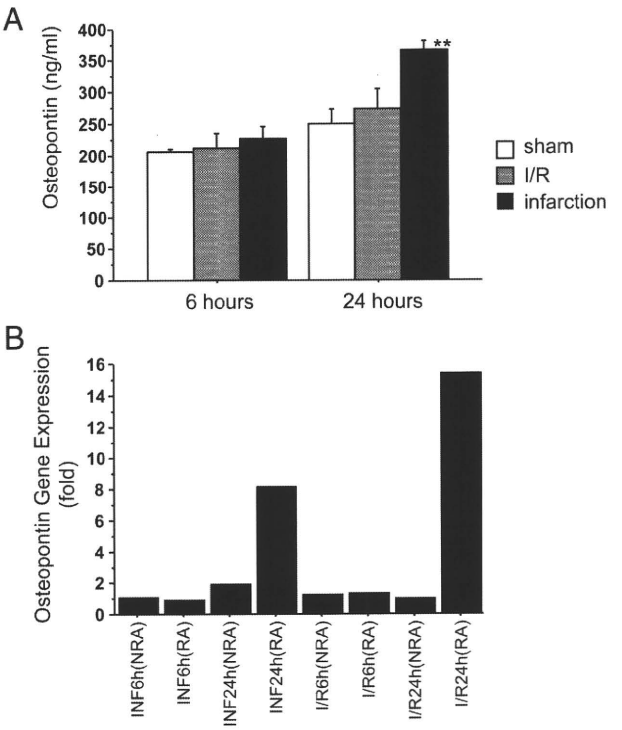

Figure 7. A, The time course of the serum osteopontin concentrations in sham, I/R, and infarction groups. The assessment of serum osteopontin by ELISA in the sham, I/R, and infarction groups after 6 and 24 hours. The serum concentrations of osteopontin after 24 hours were 365.7±14.6 ng/mL, 273.0±30.6 ng/mL, and 249.2±23.4 ng/mL in infarction, I/R, and sham groups, respectively. Error bars represent the SEM. $^{**}P<0.01$ compared with sham. B, The changes in osteopontin gene expression in the infarcted and reperfused heart. INF indicates infarction; NRA, nonrisk area; RA, risk area.

Serum Osteopontin Concentrations in Mice

Of the infarction-induced, cardiac-secreted factors that were expected to stimulate multiple liver genes, we quantified the serum levels of osteopontin by ELISA. Serum osteopontin concentration was significantly increased in the infarction group compared with the sham group ($P=0.0012$) after 24 hours (Figure 7A). In addition, the changes in osteopontin gene expression in the infarcted and reperfused heart are shown in Figure 7B.

Signaling Pathway in Primary Hepatocytes Treated With Osteopontin

To determine whether ischemia-induced, cardiac-secreted factors affected hepatic gene expression, we investigated the effects of osteopontin on primary mouse hepatocytes (supplemental Materials and Methods); 979 genes were upregulated and 734 genes were downregulated ($P<0.05$ and fold change >2.0 determined by class comparison analysis) by osteopontin in primary hepatocytes (GSE14843). The most frequent pathway processes observed among upregulated genes as determined with the use of MetaCore software are

shown in supplemental Table XII. Osteopontin upregulated signaling pathways of protein C, angiogenesis, cell adhesion, etc, which were observed in groups 2 and 3 gene clusters in the mouse liver under conditions of myocardial ischemia (Figure 4; supplemental Tables I and II). The role of osteopontin in the postulated gene network connecting the liver and heart in myocardial ischemia is shown in Figure 6. Interestingly, many of the genes included in the postulated gene network were actually activated by osteopontin ($P<0.05$ or fold change >2.0 by class comparison analysis) in primary hepatocytes. Unexpectedly, osteopontin activated *HB-EGF*, thrombospondin 1, and fibroblast growth factor, which were released from the ischemic heart (Figure 6; supplemental Table VI) in primary hepatocytes. These results indicated that these proteins were released from the liver and from the heart under conditions of myocardial ischemia through osteopontin, and an autocrine signaling pathway may exist in the liver.

Among the candidate hepatic-secreted factors under conditions of myocardial ischemia (Figure 6A; supplemental Table VIII), we quantified the levels of *VEGF-A* in the supernatants of primary hepatocytes treated with osteopontin. The concentration of *VEGF-A* measured by ELISA was significantly increased in the supernatants of primary hepatocytes treated with osteopontin (n=6) compared with the mock group (n=7; $P=0.0042$; supplemental Figure II). Thus, important factors for tissue remodeling could be released from the liver through humoral factors, such as osteopontin, that are released from the heart under conditions of myocardial ischemia.

Quantitative RTD-PCR

We performed a quantitative RTD-PCR with TaqMan probes. In the I/R group, protein C, coagulation factor X, *CNTF*, and *CSF-1* were upregulated in the liver. In the infarction group, protein C, urokinase, and *VEGF-A* were upregulated in the liver (supplemental Figure IIIA). In the hepatocytes treated with osteopontin, protein C, coagulation factor X, ciliary neurotrophic factor, *CSF-1*, urokinase, and *VEGF-A* were upregulated compared with the mock group (supplemental Figure IIIB). These results were consistent with those of cDNA microarray analyses performed in this study.

Discussion

The liver is an essential organ that synthesizes many bioactive proteins, including acute-phase inflammatory proteins (eg, C-reactive protein and IL-6) and coagulation factors. Therefore, it has been speculated that the liver may be involved in systemic reactions that modify the pathophysiology of ACS, although this possibility has not been addressed in detail.

In this study, we examined the gene expression profiles of the livers of mice affected by myocardial I/R or infarction. Marked changes in hepatic gene expression were observed after 24 hours, despite the lack of histological changes in the liver. These changes were essentially restored to normal after 3 to 7 days (data not shown). These findings may not be due to hemodynamic changes during myocardial I/R or infarction. Instead, inflammatory mediators or humoral factors released from the affected heart may be responsible for the observed alterations in hepatic gene expression. This was further confirmed by investigation of signaling pathways in primary hepatocytes induced by osteopontin, a candidate humoral factor released from the ischemic myocardium in vitro.

To exclude the possibility that these changes in gene expression were due to systemic hypotension during I/R or infarction, we performed an additional experiment involving liver I/R to examine whether a pattern of gene expression similar to that in the myocardial I/R and infarction groups could be observed in the liver. Hepatic gene expression in the liver I/R group was completely different from those in the myocardial I/R and infarction groups, with the exception of a small gene cluster (group 3). Although the group 3 gene cluster was upregulated in both the liver I/R and myocardial I/R groups at 24 hours after provocation, peak expression was delayed in the myocardial I/R group compared with the liver I/R group. A recent report of extended observations of cytokine expression in murine hepatic I/R injury indicated that the levels of expression of tumor necrosis factor-α, IL-1β, and IL-6 peaked within 4 hours and returned to baseline at 24 hours.[12] In contrast, in the myocardial I/R and infarction models, these cytokines peaked $\approx$24 to 48 hours and decreased at 7 days.[13] These findings were consistent with those of this study (data not shown). Therefore, the delayed peak of hepatic gene expression observed in this study may be correlated with the extent of inflammation in the myocardium after destruction of myocytes, rather than changes in the hemodynamic state of the liver. The lack of histological changes in the liver in the myocardial I/R and infarction models supported these suggestions, although the influence of hemodynamic state on hepatic gene expression should be carefully considered.

Interestingly, genes related to tissue remodeling, adhesion molecules, and morphogenesis were significantly upregulated in the livers of mice that were subjected to I/R or infarction. This may be related to the induction of tissue repair factors such as angiogenic or myocardiogenic factors in the heart undergoing I/R or infarction. In support of this notion, in addition to the genes upregulated during infarction, chemokines and hormonal factors, including IL-8, androgen, and estrogen receptor genes, were upregulated during I/R. These findings may reflect the presence of living myocytes and the greater release of tissue repair and bioreactive factors during I/R than during infarction.

A recent study that included a sequential analysis of ischemic mouse heart with quantitative RT-PCR demonstrated expression of IL-1β, IL-6, monocyte chemoattractant protein-1, macrophage inflammatory protein-1, and granulocyte-CSF at 6 and 24 hours.[13] These results were essentially consistent with those of our microarray analysis of pooled RNA extracted from heart specimens (data not shown).

In this study, the hepatic RNA samples were not pooled but were used to analyze the hepatic gene expression profiles individually. This strategy was successful, in that our microarray results were consistent with those produced from pooled or nonpooled liver specimens. Moreover, it facilitated the statistical evaluation of differentially expressed genes

among the various groups and revealed dynamic changes in hepatic gene expression through clustering analysis.

We analyzed the network connecting the heart-extracellular genes and liver-intracellular genes induced after I/R injury or infarction by using expression data from pooled heart samples and averaged the expression data for individual liver samples. The results suggested that factors secreted from the heart altered gene expression in the liver. By detailed analysis of signaling pathways, we identified 9 candidate genes (eg, *Osteopontin*, *HB-EGF*, *Reticulon 4*) that were upregulated in the heart and were expected to be systemically secreted and to regulate gene expression in the liver (Figure 6). Moreover, we identified the factors that were expected to be secreted from the liver induced by these signaling pathways, such as protein C, coagulation factor X, *CNTF*, *CSF-1*, and angiogenesis-related genes. These factors were expected to be systemically secreted from the liver and to modulate the pathophysiology and outcome of ACS. It has been reported that protein C prevents myocardial I/R injury,[14] *VEGF* enhances capillary density and improves cardiac function,[15] and urokinase is essential for cardiac functional recovery after acute myocardial infarction.[16]

Of the factors that were expected to be secreted from the heart, we confirmed that infarction increased the serum osteopontin concentration after 24 hours. Osteopontin is essential for the development of myocytes, tissue repair, and angiogenesis, and its downstream products, eg, polo-like kinase, were upregulated in the liver. To confirm these findings, we examined the signaling pathways in primary hepatocytes treated with osteopontin. Osteopontin activated signaling pathways of protein C, angiogenesis, and cell adhesion (supplemental Table XII) by inducing the expression of protein C, urokinase, *VEGF-A*, *CSF-1*, factor X, and ciliary neurotrophic factor (*CNTF*) in primary hepatocytes, which was confirmed by RTD-PCR or ELISA (supplemental Figures II and IIIB). Moreover, many other genes involved in the postulated gene network associating the liver and heart (Figure 6A and 6B) were actually activated in primary hepatocytes treated with osteopontin, confirming this signaling pathway. These results suggest that humoral factors play important roles in signal transduction from the ischemic myocardium to the liver.

Although our results addressed humoral factors from the heart that may affect hepatic gene expression, the effects of other factors, such as autonomic nerves, should also be considered. Because the liver has rich sympathetic and parasympathetic innervation,[17–19] it is possible that sympathetic hyperactivity affects hepatic gene expression. Although hydralazine has been reported to activate sympathetic nerves,[20,21] we observed no differences in gene expression in the hydralazine-treated group compared with the sham-operated group (data not shown). Therefore, autonomic nerves seemed to have little effect on hepatic gene expression determined in this study.

In conclusion, we reported new insights into the pathophysiology of ACS, which may facilitate identification of the mechanisms by which an acute coronary event causes systemic reactions. Further studies are needed to determine whether early therapeutic targeting of the liver during an acute coronary event has any beneficial effect on the clinical outcome in these patients.

Study Limitations

Although we confirmed that the serum osteopontin concentration was increased during myocardial ischemia, other proteins that could potentially be secreted from the heart and liver were not assayed. Further studies are needed to determine whether these proteins, including osteopontin, actually affect hepatic gene expression as observed in this study.

Acknowledgments

We thank Dr Yoh Zen (Department of Human Pathology, Kanazawa University Graduate School of Medical Science, Kanazawa, Japan) for consultation on the pathology of the liver.

Disclosures

None.

References

1. Pfohl M, Schreiber I, Liebich HM, Haring HU, Hoffmeister HM. Upregulation of cholesterol synthesis after acute myocardial infarction—is cholesterol a positive acute phase reactant? *Atherosclerosis*. 1999;142:389–393.
2. Tousoulis D, Antoniades C, Bosinakou E, Kotsopoulou M, Tsoufis C, Marinou K, Charakida M, Stefanadi E, Vavuranakis M, Latsios G, Stefanadis C. Differences in inflammatory and thrombotic markers between unstable angina and acute myocardial infarction. *Int J Cardiol*. 2007;115:203–207.
3. Busch G, Seitz I, Steppich B, Hess S, Eckl R, Schömig A, Ott I. Coagulation factor Xa stimulates interleukin-8 release in endothelial cells and mononuclear leukocytes: implications in acute myocardial infarction. *Arterioscler Thromb Vasc Biol*. 2005;25:461–466.
4. van't Veer LJ, Dai H, van de Vijver MJ, He YD, Hart AA, Mao M, Peterse HL, van der Kooy K, Marton MJ, Witteveen AT, Schreiber GJ, Kerkhoven RM, Roberts C, Linsley PS, Bernards R, Friend SH. Gene expression profiling predicts clinical outcome of breast cancer. *Nature*. 2002;415:530–536.
5. Nielsen TO, West RB, Linn SC, Alter O, Knowling MA, O'Connell JX, Zhu S, Fero M, Sherlock G, Pollack JR, Brown PO, Botstein D, van de Rijn M. Molecular characterization of soft tissue tumours: a gene expression study. *Lancet*. 2002;359:1301–1307.
6. van de Vijver MJ, He YD, van't Veer LJ, Dai H, Hart AA, Voskuil DW, Schreiber GJ, Peterse JL, Roberts C, Marton MJ, Parrish M, Atsma D, Witteveen A, Glas A, Delahaye L, van der Velde T, Bartelink H, Rodenhuis S, Rutgers ET, Friend SH, Bernards R. A gene-expression signature as a predictor of survival in breast cancer. *N Engl J Med*. 2002;347:1999–2009.
7. Hedenfalk I, Duggan D, Chen Y, Radmacher M, Bittner M, Simon R, Meltzer P, Gusterson B, Esteller M, Kallioniemi OP, Wilfond B, Borg A, Trent J, Raffeld M, Yakhini Z, Ben-Dor A, Dougherty E, Kononen J, Bubendorf L, Fehrle W, Pittaluga S, Gruvberger S, Loman N, Johannsson O, Olsson H, Sauter G. Gene-expression profiles in hereditary breast cancer. *N Engl J Med*. 2001;344:539–548.
8. Gabrielsen A, Lawler PR, Yongzhong W, Steinbrüchel D, Blagoja D, Paulsson-Berne G, Kastrup J, Hansson GK. Gene expression signals involved in ischemic injury, extracellular matrix composition and fibrosis defined by global mRNA profiling of the human left ventricular myocardium. *J Mol Cell Cardiol*. 2007;42:870–883.
9. LaFramboise WA, Bombach KL, Dhir RJ, Muha N, Cullen RF, Pogozelski AR, Turk D, George JD, Guthrie RD, Magovern JA. Molecular dynamics of the compensatory response to myocardial infarct. *J Mol Cell Cardiol*. 2005;38:103–117.
10. Giesen PL, Peltenburg HG, de Zwaan C, Janson PC, Flendrig JG, Hermens WT. Greater than expected alanine aminotransferase activities in plasma and in hearts of patients with acute myocardial infarction. *Clin Chem*. 1989;35:279–283.
11. Lu J, Getz G, Miska EA, Alvarez-Saavedra E, Lamb J, Peck D, Sweet-Cordero A, Ebert BL, Mak RH, Ferrando AA, Downing JR, Jacks T, Horvitz HR, Golub TR. MicroRNA expression profiles classify human cancers. *Nature*. 2005;435:834–838.
12. Langdale LA, Hoagland V, Benz W, Riehle KJ, Campbell JS, Liggitt DH, Fausto N. Suppressor of cytokine signaling expression with increasing

severity of murine hepatic ischemia-reperfusion injury. *J Hepatol.* 2008; 49:198–206.
13. Vandervelde S, van Luyn MJ, Rozenbaum MH, Petersen AH, Tio RA, Harmsen MC. Stem cell-related cardiac gene expression early after murine myocardial infarction. *Cardiovasc Res.* 2007;73:783–793.
14. Loubele ST, Spek CA, Leenders P, van Oerle R, Aberson HL, Hamulyák K, Ferrell G, Esmon CT, Spronk HM, ten Cate H. Activated protein C protects against myocardial ischemia/reperfusion injury via inhibition of apoptosis and inflammation. *Arterioscler Thromb Vasc Biol.* 2009;29: 1087–1092.
15. Zhang J, Ding L, Zhao Y, Sun W, Chen B, Lin H, Wang X, Zhang L, Xu B, Dai J. Collagen-targeting vascular endothelial growth factor improves cardiac performance after myocardial infarction. *Circulation.* 2009;119: 1776–1784.
16. Heymans S, Luttun A, Nuyens D, Theilmeier G, Creemers E, Moons L, Dyspersin GD, Cleutjens JP, Shipley M, Angellilo A, Levi M, Nübe O, Baker A, Keshet E, Lupu F, Herbert JM, Smits JF, Shapiro SD, Baes M, Borgers M, Collen D, Daemen MJ, Carmeliet P. Inhibition of plasminogen activators or matrix metalloproteinases prevents cardiac rupture but impairs therapeutic angiogenesis and causes cardiac failure. *Nat Med.* 1999;5:1135–1142.
17. Sasse D, Spornitz UM, Maly IP. Liver architecture. *Enzyme.* 1992; 46:8–32.
18. McCuskey RS, Reilly FD. Hepatic microvasculature: dynamic structure and its regulation. *Semin Liver Dis.* 1993;13:1–12.
19. Berthoud HR. Anatomy and function of sensory hepatic nerves. *Anat Rec A Discov Mol Cell Evol Biol.* 2004;280:827–835.
20. Yoshioka M, Togashi H, Minami M, Saito H. Effects of hydralazine on adrenal and cardiac sympathetic nerve activity in anesthetized rats. *Res Commun Chem Pathol Pharmacol.* 1986;54:313–320.
21. Johansson M, Elam M, Rundqvist B, Eisenhofer G, Herlitz H, Jensen G, Friberg P. Differentiated response of the sympathetic nervous system to angiotensin-converting enzyme inhibition in hypertension. *Hypertension.* 2000;36:543–548.

CLINICAL PERSPECTIVE

Acute coronary syndrome (ACS) is accompanied by systemic changes in inflammation, coagulation, and metabolism, which may affect the outcome and prognosis of ACS. These systemic reactions are not explained by cardiac events alone. Several lines of evidence suggest that patients with fatty liver disease have a high risk of developing cardiovascular diseases, and it is possible to speculate that the liver is involved in a systemic reaction that modifies the pathogenesis of ACS. However, the relation between liver and myocardial ischemia in the acute ischemic phase has not been elucidated so far. In this investigation, we simultaneously analyzed the gene expression profiles of the liver and heart during acute myocardial ischemia in mice and observed the presence of humoral factors that intervened between the heart and liver. These humoral factors were released from the heart and influenced the liver to secrete important tissue remodeling factors. One of these humoral factors, osteopontin, a widely expressed glycoprotein, was increased in the ischemic heart and altered the gene expression of hepatocytes to produce important tissue remodeling factors (such as vascular endothelial growth factor-A). Our observations suggest that hepatic gene expression is potentially regulated by humoral factors of cardiac origin provoked by myocardial ischemia, and we provide direct evidence that the liver is involved in a systemic reaction that accompanies ACS. Our findings provide potential new insights into the pathophysiology of ACS.

Genomics 95 (2010) 217–223

Contents lists available at ScienceDirect

Genomics

journal homepage: www.elsevier.com/locate/ygeno

Comprehensive gene expression analysis of 5′-end of mRNA identified novel intronic transcripts associated with hepatocellular carcinoma

Yuji Hodo [a], Shin-ichi Hashimoto [b], Masao Honda [a], Taro Yamashita [a], Yutaka Suzuki [c], Sumio Sugano [c], Shuichi Kaneko [a,*], Kouji Matsushima [b]

[a] Department of Gastroentelorogy, Kanazawa University Graduate School of Medical Science, 13-1 Takara-Machi, Kanazawa, Ishikawa 920-8641, Japan
[b] Department of Molecular Preventive Medicine, School of Medicine, The University of Tokyo, 7-3-1, Hongo, Bunkyo-ku, Tokyo 113-0033, Japan
[c] Department of Medical Genome Sciences, Graduate School of Frontier Sciences, The University of Tokyo, 5-1-5, Kashiwanoha, Kashiwa, Chiba 277-8562, Japan

ARTICLE INFO

Article history:
Received 1 June 2009
Accepted 14 January 2010
Available online 21 January 2010

Keywords:
5′-end serial analysis of gene expression
Transcriptional start site
Acyl-coenzyme A oxidase 2
Intron
Hepatocellular carcinoma

ABSTRACT

To elucidate the molecular feature of human hepatocellular carcinoma (HCC), we performed 5′-end serial analysis of gene expression (5′SAGE), which allows genome-wide identification of transcription start sites in addition to quantification of mRNA transcripts. Three 5′SAGE libraries were generated from normal human liver (NL), non-B, non-C HCC tumor (T), and background non-tumor tissues (NT). We obtained 226,834 tags from these libraries and mapped them to the genomic sequences of a total of 8,410 genes using RefSeq database. We identified several novel transcripts specifically expressed in HCC including those mapped to the intronic regions. Among them, we confirmed the transcripts initiated from the introns of a gene encoding acyl-coenzyme A oxidase 2 (*ACOX2*). The expression of these transcript variants were up-regulated in HCC and showed a different pattern compared with that of ordinary *ACOX2* mRNA. The present results indicate that the transcription initiation of a subset of genes may be distinctively altered in HCC, which may suggest the utility of intronic RNAs as surrogate tumor markers.

Introduction

Hepatocellular carcinoma (HCC) is the fifth most common cancer worldwide and the third most common cause of cancer mortality. HCC usually develops in patients with virus-induced (e.g., hepatitis B virus (HBV) and hepatitis C virus (HCV)) chronic inflammatory liver disease [1]; however, non-B, non-C HCC has been reported in patients negative for both HBV and HCV [2]. HCC development is a multistep process involving changes in host gene expression, some of which are correlated with the appearance and progression of a tumor. Multiple studies linking hepatitis viruses and chemical carcinogens with hepatocarcinogesis have provided insights into tumorigenesis [1,3]. Nevertheless, the genetic events that lead to HCC development remain unknown, and the molecular pathogenesis of HCC in most patients is still unclear. Therefore, elucidation of the genetic changes specific to the pathogenesis of non-B, non-C HCC may be useful to reveal the molecular features of HCCs irrelevant to viral infection.

Gene expression profiling, either by cDNA microarray [4] or serial analysis of gene expression (SAGE) [5], is a powerful molecular technique that allows analysis of the expression of thousands of genes. In particular, SAGE enables the rapid, quantitative, and simultaneous monitoring of the expression of tens of thousands of genes in various tissues [6,7]. Although numerous studies using cDNA microarrays and SAGE have been performed to clarify the genomic and molecular alterations associated with HCC [6,8–10], most expression data have been derived from the 3′-end region of mRNA. Recent advances in molecular biology have enabled genome-wide analysis of the 5′-end region of mRNA that revealed the variation in transcriptional start sites [11,12] and the presence of a large number of non-coding RNAs [13]. These approaches might be useful for identifying the unique and undefined genes associated with HCC not identified by the analysis of the 3′-end region of mRNA. SAGE based on the 5′-end (5′SAGE), a recently developed technique, allows for a comprehensive analysis of the transcriptional start site and quantitative gene expression [14]. This article is to elucidate the molecular carcinogenesis of non-B, non-C HCCs, while those heterogeneous entities are supposed not to share the same etiology, by using 5′SAGE.

Results

Annotation of the 5′SAGE tags to the human genome

We characterized a total of 226,834 tags from three unique 5′SAGE libraries (75,268 tags from the normal liver (NL) library, 75,573 tags from the non-tumor tissue (NT) library, and 75,993 tags from the tumor (T) library) and compared them against the human genome

Abbreviations: 5′SAGE, 5′-end serial analysis of gene expression; HCC, hepatocellular carcinoma; ACOX2, acyl-coenzyme A oxidase 2.

* Corresponding author. Fax: +81 76 234 4250
E-mail address: skaneko@m-kanazawa.jp (S. Kaneko).

0888-7543/$ – see front matter © 2010 Elsevier Inc. All rights reserved.
doi:10.1016/j.ygeno.2010.01.004

sequence. A total of 211,818 tags matched genomic sequences, representing 104,820 different tags in the three libraries (Table 1). About 60–65% of these tags mapped to a single locus in the genome in each library. Then, we mapped these single-matched tags to the well-annotated genes using RefSeq database (www.ncbi.nlm.nih.gov/RefSeq/, reference sequence database developed by NCBI). A total of 45,601 tags from the NL library, 39,858 from the NT library, and 41,265 from the T library were successfully mapped to 8410 unique genes (4397 genes detected in the NL library, 5194 genes in the NT library, and 6304 genes in the T library).

Gene expression profiling of non-B, non-C HCC

Abundantly expressed transcripts in the NL library and their corresponding expression in the NT and T libraries are shown in Table 2. The most abundant transcript in all three libraries was encoded by the *albumin (ALB)* gene. Transcripts encoding apolipoproteins were also abundantly expressed in each library, suggesting the preservation of hepatocytic gene expression patterns in HCC. Of note, the expression of *haptoglobin (HP)* (NL: 631, NT: 329, T: 57) and *metallothionein 1G (MT1G)* (NL: 392, NT: 169, T: 2) was decreased in the NT library and more in T library compared with NL library. Furthermore, the expression of *metallothionein 2A (MT2A)* (NL: 1027, NT: 872, T: 19), *metallothionein 1X (MT1X)* (NL: 547, NT: 644, T: 11), and *metallothionein 1E (MT1E)* (NL: 275, NT: 340, T: 2) was decreased almost fifty-fold or more in the T library compared with the NL and NT libraries. In contrast, the expression of *ribosomal protein S29 (RPS29)* (NL: 372, NT: 1011, T: 1768) was increased in the NT library and more in T library compared with NL library. Thus, transcripts associated with a certain liver function including xenobiotic metabolism might be suppressed whereas those associated with protein synthesis might be expressed in non-B, non-C HCC, similar to that observed in HCV-HCC [15].

We then investigated the characteristics of gene expression patterns in non-B, non C HCC. Two hundred fifty-four and 172 genes were up- or down-regulated in the T library more than five-fold compared with the NL library (data not shown). The top 10 genes are listed in Table 3a, and we identified several novel genes not yet reported to be differentially expressed in non-B, non-C HCC. Representative novel gene expression changes identified by 5′SAGE were validated by semi-quantitative reverse transcriptase-polymerase chain reaction (RT-PCR) analysis (Supplemental Fig. 1). RT-PCR results showed that the expression of *galectin 4 (LGALS4)*, *X antigen family, member 1A (XAGE 1A)*, *retinol dehydrogenase 11 (RDH11)*, *hydroxysteroid (17-beta) dehydrogenase 14 (HSD17B14)* *transmembrane 14A (TMEM14A)*, *stimulated by retinoic acid 13 homolog (STRA13)*, and *dual specificity phosphatase 23 (DUSP23)* was increased, whereas the expression of *C-type lectin superfamily 4 member G (CLEC4G)* was decreased in HCC tissues compared with the non-tumor tissues.

To further characterize the gene expression patterns of non-B, non-C HCC comprehensively, we compared the Gene Ontology process of three types of HCCs (i.e., non-B, non-C HCC; HBV-HCC; HCV-HCC) based on our previously described data [16]. The pathway analysis using MetaCore™ software showed that the immune related and cell adhesion related pathways were up-regulated in HCV-HCC with statistically significance, and the insulin signaling and angiogenesis related pathways were up-regulated in HBV-HCC with statistically significance, confirming our previous results [16]. Interestingly, genes associated with progesterone signaling were up-regulated in non-B, non-C HCC, while genes associated with proteolysis in the cell cycle, apoptosis and the ESR1-nuclear pathway were up-regulated in all types of HCC (Supplemental Fig. 2).

Dynamic alteration of transcription initiation in HCC

Although various transcriptome analyses have discovered considerable gene expression changes in cancer, it is still unclear if transcription is differentially initiated and/or terminated in HCC compared with the non-cancerous liver. We therefore explored the characteristics of transcription initiation and/or termination in HCC using 5′SAGE and 3′SAGE data. Markedly, we observed relevant differences between 5′ SAGE and 3′SAGE data derived from the same HCC sample (Tables 3a and b). For example, a gene encoding *coagulation factor XIII, B polypeptide (F13B)* was 13-fold up-regulated at transcription start sites (5′SAGE) but two-fold down-regulated at transcription termination sites (3′SAGE). On the other hand, a gene encoding *adenylate cyclase 1 (ADCY1)* was 50-fold down-regulated at transcriptional termination sites (3′SAGE) but showed no difference at transcriptional start sites (5′SAGE). These data suggest the dramatic alteration of all process of transcription in HCC, and the transcripts initiated at certain sites might be specifically associated with and involved in HCC pathogenesis, which could be a novel marker for HCC diagnosis.

Identification of novel intronic transcripts in HCC

Recent lines of evidence suggest that the majority of sequences of eukaryotic genomes may be transcribed, not only from known transcription start sites but also from intergenic regions and introns [17,18]. Introns are recognized as a significant source of functional non-coding RNAs (ncRNAs) including microRNAs (miRNAs) [18]. Moreover, a recent report implied the role of some large intronic RNAs in the pathogenesis of several types of malignancies [19]. Thus, analysis of transcripts originating from introns might be valuable for elucidating the genetic traits of HCC. We therefore focused on the transcriptional start sites potentially initiated from the intron and deregulated in HCC using 5′SAGE data. We identified that 97% of 5′ SAGE tags annotated by the RefSeq database matched the sequences in the exons, while 3% matched those in the introns (1257 in the N library, 1225 in the NT library, and 1261 in the T library) (Table 4a). To identify the possible promoter regions located in the intron, we clustered the different SAGE tags to a certain genomic region if these tags positioned within 500 bp intervals (Supplemental Fig. 3), as described previously [12].

Table 1
Experimental matching of 5′SAGE tags to genome.

	Normal liver	Non-tumor	Tumor	Total
All tags	75,268	75,573	75,993	226,834
Tags mapped to genome (%)				
1 locus/genome	51,076 (71.2)	47,200 (68.0)	48,503 (68.5)	146,779 (69.3)
Multiple loci/genome	20,608 (28.8)	22,142 (32.0)	22,289 (31.5)	65,039 (30.7)
Total tags	71,684 (100)	69,342 (100)	70,792 (100)	211,818 (100)
Unique tags mapped to genome (%)				
1 locus/genome	20,736 (65.5)	20,487 (60.2)	23,753 (60.7)	64,976 (62.0)
Multiple loci/genome	10,914 (34.5)	13,548 (39.8)	15,382 (39.3)	39,844 (38.0)
Total tags	31,650 (100)	34,035 (100)	39,135 (100)	104,820 (100)
Total tags to RefSeq	45,601	39,858	41,265	126,724
Unique gene	4397	5194	6304	8410

5′SAGE indicates 5′-end serial analysis of gene expression.

Table 2
The highly expressed genes in the NL library and corresponding expression in the NT and T libraries (top 50 from NL library).

Tag count			Ratio		Gene
NL	NT	T	NT/NL	T/NL	
3731	1716	2328	0.460	0.624	Albumin (ALB)
2484	2146	2042	0.864	0.822	Apolipoprotein C-I (APOC1)
1955	1603	1079	0.820	0.552	Apolipoprotein A-II (APOA2)
1653	1050	828	0.635	0.501	Apolipoprotein A-I (APOA1)
1252	1908	1203	1.524	0.961	Transthyretin (prealbumin, amyloidosis type I) (TTR)
1233	724	220	0.587	0.178	Serpin peptidase inhibitor, clade A, member 1 (SERPINA1)
1027	872	19	0.849	0.019	Metallothionein 2A (MT2A)
755	1144	762	1.515	1.009	Ferritin, light polypeptide (FTL)
713	632	680	0.886	0.954	Alpha-1-microglobulin/bikunin precursor (AMBP)
635	524	1336	0.825	2.104	Apolipoprotein E (APOE)
631	329	57	0.521	0.090	Haptoglobin (HP)
600	228	212	0.380	0.353	Fibrinogen gamma chain (FGG)
549	395	302	0.719	0.550	Apolipoprotein C-III (APOC3)
547	644	11	1.177	0.020	Metallothionein 1X (MT1X)
479	257	290	0.537	0.605	Tumor protein, translationally-controlled 1 (TPT1)
463	217	53	0.469	0.114	Serpin peptidase inhibitor, clade A, member 3 (SERPINA3)
393	204	206	0.519	0.524	Ribosomal protein L26 (RPL26)
392	169	2	0.431	0.005	Metallothionein 1G (MT1G)
372	1011	1768	2.718	4.753	Ribosomal protein S29 (RPS29)
306	163	223	0.533	0.729	Ribosomal protein S27 (RPS27)
279	135	159	0.484	0.570	Ribosomal protein S16 (RPS16)
275	340	2	1.236	0.007	Metallothionein 1E (MT1E)
269	170	246	0.632	0.914	Ribosomal protein S23 (RPS23)
260	142	92	0.546	0.354	Fibrinogen beta chain (FGB)
260	200	195	0.769	0.750	Aldolase B, fructose-bisphosphate (ALDOB)
255	228	286	0.894	1.122	Ribosomal protein S12 (RPS12)
248	162	198	0.653	0.798	Ribosomal protein S14 (RPS14)
246	175	70	0.711	0.285	Interferon induced transmembrane protein 3 (IFITM3)
239	198	273	0.828	1.142	Ribosomal protein L31(RPL31)
229	264	0	1.153	0.004	Hepcidin antimicrobial peptide (HAMP)
228	149	156	0.654	0.684	Ribosomal protein S20 (RPS20)
222	191	117	0.860	0.527	Ubiquitin B (UBB)
216	218	352	1.009	1.630	Ribosomal protein L41 (RPL41)
210	150	155	0.714	0.738	Ribosomal protein, large, P1(RPLP1)
201	110	90	0.547	0.448	Ribosomal protein, large, P2 (RPLP2)
198	102	64	0.515	0.323	Fibrinogen alpha chain (FGA)
196	143	408	0.730	2.082	Ribosomal protein L37 (RPL37)
192	123	56	0.641	0.292	Ribosomal protein L37a (RPL37A)
191	208	346	1.089	1.812	Ribosomal protein L30 (RPL30)
174	109	76	0.626	0.437	Ribosomal protein L35 (RPL35)
169	208	3	1.231	0.018	Cytochrome P450, family 2, subfamily E, polypeptide 1 (CYP2E1)
167	105	300	0.629	1.796	Apolipoprotein H (beta-2-glycoprotein I) (APOH)
162	106	33	0.654	0.204	Serum amyloid A4, constitutive (SAA4)
159	85	157	0.535	0.987	Ribosomal protein L34 (RPL34)
159	113	229	0.711	1.440	Transferrin (TF)
155	84	135	0.542	0.871	Ribosomal protein S11 (RPS11)
152	125	101	0.822	0.664	Ribosomal protein S13 (RPS13)
147	84	1	0.571	0.007	Nicotinamide *N*-methyltransferase (NNMT)
147	180	35	1.224	0.238	Hemopexin (HPX)
146	89	121	0.610	0.829	Alpha-2-HS-glycoprotein (AHSG)

To avoid division by 0, a tag value of 1 for any tag that was not detectable was used.
NL, normal liver; NT, non-tumor; T, tumor.

More than 2 tags were detected in the intronic regions of the 164 genes in the NL, 168 genes in the NT, and 157 genes in the T library, suggesting that these regions might be potential intronic promoter regions (Table 4a). The biological process of these intron-origin transcripts using Human Protein Reference Database (http://www.hprd.org/) showed that these were related to basic cellular functions such as signal transduction, transport, and regulation of the nucleobase and nucleotide, suggesting that these intronic transcripts

Table 3a
Differently expressed genes in HCC (top 10 from 5′SAGE).

5′SAGE	3′SAGE	5′/3′	Gene
T/NL	T/NL	Ratio	
Up-regulated gene			
19	6	3.17	P antigen family, member 2 (prostate associated) (PAGE2)
18	10	1.8	Lectin, galactoside-binding, soluble, 4 (LGALS4)
16	3	5.33	Choline phosphotransferase 1 (CHPT1)
14	2	7	X antien family, member 1A (XAGE1A)
14	2	7	Dehydrogenase/reductase (SDR family) member 4 (DHRS4)
14	2	7	Sterol-C5-desaturase-like (SC5DL)
13	0.5	26	Coagulation factor XIII, B polypeptide (F13B)
13	2.33	5.58	Retinol dehydrogenase 11 (all-trans and 9-cis) (RDH11)
13	0.5	26	Transmembrane protein 14A (TMEM14A)
12	1.33	9.02	Dual specificity phosphatase 23 (DUSP23)
Down-regulated gene			
0.00436	0.0137	0.318	Hepcidin antimicrobial peptide (HAMP)
0.0051	ND		Metallothionein 1G (MT1G)
0.0068	0.04	0.17	Nicotinamide *N*-methyltransferase (NNMT)
0.00727	ND		Metallothionein 1E (functional) (MT1E)
0.0098	0.0526	0.186	C-reactive protein, pentraxin-related (CRP)
0.0145	ND		Metallothionein 1 M (MT1M)
0.0152	ND		Phospholipase A2, group IIA (platelets, synovial fluid) (PLA2G2A)
0.0178	0.111	0.16	Cytochrome P450, family 2, subfamily E, polypeptide 1 (CYP2E1)
0.0185	0.192	0.096	Metallothionein 2A (MT2A)
0.0201	ND		Metallothionein 1X (MT1X)

3′SAGE, 3′-end serial analysis of gene expression; 5′SAGE, 5′-end serial analysis of gene expression; HCC, hepatocellular carcinoma; NL, normal liver; T, tumor.

may play a fundamental role in the liver (data not shown). Among these genes, 12 were differentially expressed between the NL and T libraries more than four-fold (Table 4b). Interestingly, intronic transcripts (determined by 5′SAGE) of genes encoding *SAMD3*,

Table 3b
Differently expressed genes in HCC (top 10 from 3′SAGE).

5′SAGE	3′SAGE	5′/3′	Gene
T/NL	T/NL	Ratio	
Up-regulated gene			
ND	15		Leukocyte immunoglobulin-like receptor, subfamily B, member 1 (LILRB1)
ND	12		Fibroblast growth factor 5 (FGF5)
1	11	0.909	Adenosine deaminase, tRNA-specific 1 (ADAT1)
5	11	0.454	px19-like protein (PRELID1)
4.4	11	0.4	Anaphase promoting complex subunit 11 (ANAPC11)
ND	10.3		Chromosome 21 open reading frame 77 (C21orf77)
ND	10		von Willebrand factor (VWF)
2.333	10	0.233	ATX1 antioxidant protein 1 homolog (yeast) (ATOX1)
18	10	1.8	Lectin, galactoside-binding, soluble, 4 (LGALS4)
ND	9.5		Solute carrier family 26 (sulfate transporter), member 2 (SLC26A2)
Down-regulated gene			
0.5	0.012	41.7	ELL associated factor 1 (EAF1)
0.5	0.0137	36.5	TGF beta-inducible nuclear protein 1 (NSA2)
0.000436	0.0137	0.032	Hepcidin antimicrobial peptide (HAMP)
1	0.0179	55.9	Basic, immunoglobulin-like variable motif containing (BIVM)
ND	0.0182		DNA fragmentation factor, 45 kDa, alpha polypeptide (DFFA)
1	0.0185	54.1	GRIP1 associated protein 1 (GRIPAP1)
ND	0.0189		Nuclear factor of activated T-cells 5, tonicity-responsive (NFAT5)
1	0.0204	49	Adenylate cyclase 1 (ADCY1)
0.333	0.0312	10.7	Dihydroorotate dehydrogenase (DHODH)
0.738	0.0312	23.7	Ribosomal protein, large, P1 (RPLP1)

3′SAGE, 3′-end serial analysis of gene expression; 5′SAGE, 5′-end serial analysis of gene expression; HCC, hepatocellular carcinoma; NL, normal liver; T, tumor.

Table 4a
Number of 5′SAGE tags mapped to intronic region.

	NL	NT	T
Tag mapped to intron	1287	1253	1292
Total promoter region	952	981	1020
(tag number = 1)	788	813	863
(tag number ≧2)	164	168	157

ACOX2, *HGD*, *CYP3A5*, *KNG1* and *AGXT* were increased, while their 3′ transcripts (determined by 3′SAGE) were decreased in HCC. In contrast, both 5′ intronic transcripts and 3′ transcripts encoding *HFM1*, *SERPINA1*, *SUPT3H*, *A2M* and *TMEM176B* were similarly decreased in HCC. Taken together, these data imply that the canonical- and intronic-promoter activities of a subset of genes including *SAMD3*, *ACOX2*, *HGD*, *CYP3A5*, *KNG1* and *AGXT* might be differently regulated in HCC.

ACOX2 as a novel intronic gene deregulated in HCC

A subset of genes listed above may be transcribed from intronic regions specifically in HCC. Among these genes, we focused on the regulation of *ACOX2*, which is reported to be potentially involved in peroxisomal beta-oxidation and hepatocarcinogenesis [20]. The intron-origin expression of *ACOX2* increased six-fold in HCC compared with the NT by 5′SAGE, while the expression based on the 3′end was almost similar between HCC and NT lesions (Table 4b). Close examination of 5′SAGE data identified two potential intron-origin transcripts of *ACOX2* (Supplemental Fig. 4). The first (intronic-*ACOX2-1*) was initiated upstream of the tenth exon, whereas the second (intronic-*ACOX2-2*) was initiated upstream of the twelfth exon of *ACOX2* (Supplemental Fig. 4). The sequence of the intronic part was unique, and the remaining part of the sequence was shared with the canonical transcripts of *ACOX2*.

The expression of canonical *ACOX2* and the two types of intron-origin transcripts was investigated in NL, NT, and T tissues by RT-PCR (Fig. 1A). Although canonical *ACOX2* expression was decreased in T than in NL, the intron-origin transcript, particularly intronic-*ACOX2-1*, was increased in T. Intronic-*ACOX2-2* transcripts also showed a modest increase. We further evaluated the alteration of these transcripts in 19 HBV-HCCs, 20 HCV-HCCs, and 4 non-B, non-C HCCs, and their background liver tissues by canonical *ACOX2* and intronic-*ACOX2* specific real-time detection (RTD)-PCR. Although the expression of canonical *ACOX2* was decreased, the expression of intronic-*ACOX2* was significantly increased (Fig. 1B). Importantly, the gene expression ratios of intronic-to canonical *ACOX2* increased more in moderately differentiated HCCs (mHCC) than in well-differentiated HCCs (wHCC), suggesting the involvement of intronic-*ACOX2* expression on HCC progression.

Table 4b
Differentially expressed intronic promoter regions in HCC.

5′SAGE T/NL	3′SAGE T/NL	5′/3′ Ratio	Gene
Up-regulated			
9	1	9.00	Sterile alpha motif domain containing 3 (SAMD3)
6	0.89	6.74	Acyl-Coenzyme A oxidase 2, branched chain (ACOX2)
6	0.62	9.68	Homogentisate 1,2-dioxygenase (homogentisate oxidase) (HGD)
6	0.009	666.67	Cytochrome P450, family 3, subfamily A, polypeptide 5 (CYP3A5)
5	0.64	7.81	Kininogen 1 (KNG1)
4	0.36	11.11	Alanine-glyoxylate aminotransferase (AGXT)
4	1	4.00	Crystallin, alpha A (CRYAA)
Down-regulated			
0.13	1	0.13	HFM1, ATP-dependent DNA helicase homolog (*S. cerevisiae*) (HFM1)
0.25	0.51	0.49	Serpin peptidase inhibitor, clade A member 1 (SERPINA1)
0.25	1	0.25	Suppressor of Ty 3 Homolog (*S. cerevisiae*) (SUPT3H)
0.25	0.2	1.25	Alpha-2-macroglobulin (A2M)
0.25	0.083	3.13	Transmembrane protein 176B (TMEM176B)

3′SAGE, 3′-end serial analysis of gene expression; 5′SAGE, 5′-end serial analysis of gene expression; HCC, hepatocellular carcinoma; NL, normal liver; NT, non-tumor; T, tumor.

Discussion

This is the first comprehensive transcriptional analysis of tissue lesions of non-B, non-C HCC, background liver and NL using the 5′ SAGE method. Approximately 6.7% of our 5′SAGE tags showed no matching within the human genome, possibly due to the presence of a single nucleotide polymorphism (SNP) in the human genome. Out of the complete matched tags in the genome, 70% were assigned to unique positions and 30% to two or more loci. The tags with multiple matches with genomic loci were largely retrotransposon elements, repetitive sequences, and pseudogenes.

In this study, the analysis of non-B, non-C HCC enabled us to evaluate direct molecular changes associated with HCC without any bias of gene induction by virus infection. The gene expression profile based on our 5′SAGE tags revealed that *albumin (ALB)* and apolipoproteins were highly expressed in NL, indicating the massive production of plasma proteins in NL; these results are similar to those of our previous study using 3′SAGE [6]. Other genes such as *aldolase B (ALDOB)*, *antitrypsin (SERPINA1)*, and *haptoglobin (HP)* were also highly expressed in NL, in both the 5′SAGE and 3′SAGE libraries (Table 2) [6]. Comparison of the expression profiles among NL, background NT and T identified several differentially expressed transcripts in T. *Galectin-4 (LGALS4)* was up-regulated and *HAMP*, *NNMT*, *CYP2E1*, and *metallothionein* were down-regulated in HCC in accordance with previous findings (Table 3a) [8,9,21]. Moreover, *CLEC4G*, which was predominantly expressed in the sinusoidal endothelial cells of the liver, was down-regulated in HCC. In addition, we first found that *P antigen family, member 2 (PAGE2)* and *XAGE1A* were up-regulated in HCC (Table 3a, Supplemental Fig. 1). These genes were members of cancer-testis antigen that include MAGE-family genes. MAGE-family members were originally found to be up-regulated in HCV-related HCC, and reported to be useful as molecular markers and as possible target molecules for immunotherapy in human HCC [22]. In this study, we identified that these members of genes were also up-regulated in non B, non-C HCC. Thus, these genes may be useful as molecular markers and therapeutic targets for the treatment of a certain type of human HCC.

There existed some discrepancy between 5′SAGE and 3′SAGE results, even though they were derived from the same sample. Technical issues such as amplication error, difference of restriction enzyme, and annotation error have been described previously [14]. It is possible that 3′ transcripts might be more stable than 5′ transcripts by binding of ribosomal proteins during translation. Another possibility is the diversity of the transcriptional start and/or termination sites. One of the advantages of 5′SAGE analysis is the potential to determine the transcriptional start sites in each gene. Indeed, a recent study indicated the importance of an insulin splice variant in the pathogenesis of insulinomas [23]. Considering the diversity of 5′ends of genes, it is more appropriate to perform 5′SAGE in combination with 3′SAGE when determining the frequency of gene expression and identifying novel transcript variants.

Here, we were able to identify at least 12 intron-origin transcripts that were differentially expressed in HCC compared with the background liver or NL. These transcripts could not be identified by the 3′SAGE approach. We also performed detailed expression analysis of *ACOX2* that was involved in the beta-oxidation of peroxisome. We

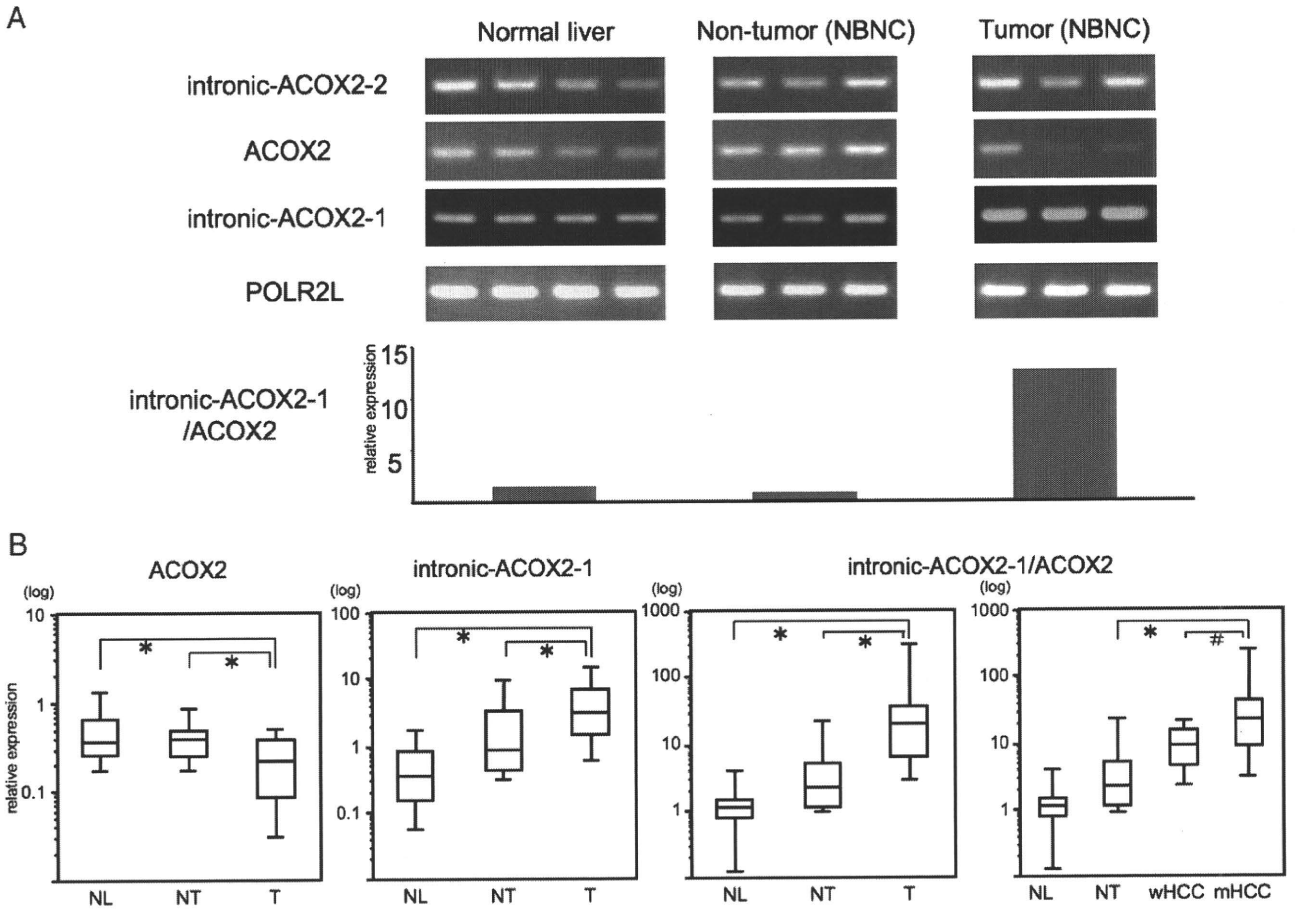

Fig. 1. (A) RT-PCR results of *ACOX2* and *ACOX2* intronic RNAs in independent NL, NT (non-B, non-C), and T (non-B, non-C) samples. RT-PCR was performed in triplicate for each sample-primer set from cDNA. The PCR products were semi-quantitatively analyzed with ImageJ software and calculated as levels relative to *polymerase (RNA) II (DNA directed) polypeptide L* (*POLR2L*). The bar graph indicates the expression ratio of intronic-ACOX2-1 to canonical ACOX2. The expression pattern of intron 1 was different from that of canonical *ACOX2*. (B) RTD-PCR analysis of *ACOX2* and *ACOX2* intronic RNAs in NL, T (HBV-related, HCV-related, and non-B, non-C), and NT tissues. Quantitative RTD-PCR was performed in duplicate for each sample-primer set from cDNA. Each sample was normalized relative to *POLR2L*. All HCC tissues were pathologically diagnosed as well differentiated HCC (wHCC) or moderately differentiated HCC (mHCC). Kruskal–Wallis tests and Mann–Whitney *U* tests were used for statistical analysis. ACOX2, acyl-Coenzyme A oxidase 2; HCC, hepatocellular carcinoma; NL, normal liver; NT, non-tumor; RT-PCR, reverse transcriptase-polymerase chain reaction; RTD-PCR, real-time detection-PCR; T, tumor. $*P<0.01$, $\#P<0.05$.

were able to clone the intron-origin *ACOX2* RNAs (intronic-*ACOX2-1, 2*) for the first time and found that intronic-*ACOX2-1* was significantly overexpressed in T compared with NT and NL. The ratio of intronic-*ACOX2-1* and canonical *ACOX2* (relative intronic-*ACOX2*) was progressively up-regulated from NL via the background liver to HCC. Importantly, the expression of relative intronic-*ACOX2* was more up-regulated in moderately differentiated HCC than in well-differentiated HCC. The intronic difference in expression might be due to a polymorphism, since the 5′SAGE library for NL and T were from different people. The mechanisms of stepwise increase of intronic-*ACOX2* in the process of hepatocarinogenesis should be clarified in future.

ACOX2 is a rate-limiting enzyme of branched-chain acyl-CoA oxidase involved in the degradation of long branched fatty acid and bile acid intermediates in peroxisomes. *ACOX2* expression was associated with the differentiation state of hepatocytes and was repressed under the undifferentiated phase of human hepatoma cell lines [24]. A decreased *ACOX2* expression was also reported in prostate cancer [25]. Here, the expression of canonical *ACOX2* was decreased, while that of intronic-*ACOX2-1* was increased in HCC. The deduced amino acid of intronic-*ACOX2-1* encodes the C-terminal (from 386 to 681 amino acids) of canonical *ACOX2*, lacking the active sites for FAD binding and a fatty acid as the substrate, suggesting that the protein may be functionally departed [26]. The biological role of the increased intronic-*ACOX2-1* was not clear, but it might be reflected by the activation of peroxisome proliferators-activated receptor alpha (PPARA). It is reported that mice lacking ACOX1, another rate-limiting enzyme in peroxisomal straight-chain fatty acid oxidation, developed steatosis and HCC characterized by increased mRNA and protein expression of genes regulated by PPARα [27]. The importance of PPARα activation in HCC development has been recently reported using HCV core protein transgenic mice [28]. Moreover, the overexpression of alpha-methylacyl-CoA racemase (AMACR), an enzyme for branched-chain fatty acid beta-oxidation, is reported to be a reliable diagnostic marker of prostate cancer and is associated with the decreased expression of ACOX2 [25]. Therefore, the expression of intronic-*ACOX2-1* might open the door for further investigations of their potential clinical use, e.g., serving as diagnostic markers of HCC, although the functional relevance of this gene should be further clarified.

In conclusion, we report the first comprehensive transcriptional analysis of non-B, non-C HCC, NT background liver, and NL tissue, based on 5′SAGE. This study offers new insights into the transcriptional changes that occur during HCC development as well as the molecular mechanism of carcinogenesis in the liver. The results suggest the presence of unique intron-origin RNAs that are useful as diagnostic markers and may be used as new therapeutic targets.

Material and methods

Samples

Samples were obtained from a 56-year-old man who had undergone surgical hepatic resection for the treatment of solitary HCC. Serological tests for hepatitis B surface (HBs) antigen and anti-HCV antibodies were negative. Tumor (T) and non-tumor (NT) tissue samples were separately obtained from the tumorous parts (diagnosed as moderately differentiated HCC) and non-tumorous parts (diagnosed as mild chronic hepatitis: F1A1) of the resected tissue. We also obtained five normal liver (NL) tissue samples from five patients who had undergone surgical hepatic resection because of metastatic liver cancer. None of the patients was seropositive for both HBs antigen and anti-HCV antibodies. Neither heavy alcohol consumption nor the intake of chemical agents was observed before surgical resection. All laboratory values related to hepatic function were within the normal range. All procedures and risks were explained verbally and provided in a written consent form.

We additionally used independent four NL tissue samples, 19 HBV-HCCs, 20 HCV-HCCs and 4 non-B, non-C HCCs, and their background liver tissue samples for reverse transcriptase-polymerase chain reaction (RT-PCR) and real-time detection (RTD)-PCR (Supplemental Table 1). Four non-B, non-C HCCs were histologically diagnosed as moderately differentiated HCCs, and the adjacent non-cancerous liver tissues were diagnosed as a normal liver, a chronic hepatitis, a pre-cirrhotic liver and a cryptogenic liver cirrhosis, respectively. None of the patients was seropositive for HBs antigen, anti-HBs antibodies, anti-hepatitis B core (HBc) antibodies and anti-HCV antibodies. Neither heavy alcohol consumption nor the intake of chemical agents was observed. Histological grading of the tumor was evaluated by two independent pathologists as described previously [16].

Generation of the 5′ SAGE library

5′SAGE libraries were generated as previously described [14]. Five to ten micrograms of poly(A)+RNA was treated with bacterial alkaline phosphatase (BAP; TaKaRa, Otsu, Japan). Poly(A)+RNA was extracted twice with phenol: chloroform (1:1), ethanol precipitated, and then treated with tobacco acid pyrophosphatase (TAP). Two to four micrograms of the BAP-TAP-treated poly(A)+RNA was divided into two aliquots and an RNA linker containing recognition sites for *Eco*RI/*Mme*I was ligated using RNA ligase (TaKaRa): one aliquot was ligated to a 5′-oligo 1 (5′-GGA UUU GCU GGU GCA GUA CAA CGA AUU CCG AC-3′) linker, and the other aliquot was ligated to a 5′-oligo 2 (5′-CUG CUC GAA UGC AAG CUU CUG AAU UCC GAC-3′) linker. After removing unligated 5′-oligo, cDNA was synthesized using RNaseH-free reverse-transcriptase (Superscript II, Invitrogen, Carlsbad, CA, USA) at 12 °C for 1 h and 42 °C for the next hour, using 10 pmol of dT adapter-primer (5′-GCG GCT GAA GAC GGC CTA TGT GGC CTT TTT TTT TTT TTT TTT-3′). After first-strand synthesis, RNA was degraded in 15 mM NaOH at 65 °C for 1 h. cDNA was amplified in a volume of 100 μl by PCR with 16 pmol of 5′ (5′ [biotin]-GGA TTT GCT GGT GCA GTA CAA-3′ or 5′[biotin]-CTG CTC GAA TGC AAG CTT CTG-3′) and 3′ (5′-GCG GCT GAA GAC GGC CTA TGT-3′) PCR primers. cDNA was amplified using 10 cycles at 94 °C for 1 min, 58 °C for 1 min, and 72 °C for 2 min. PCR products were digested with the *Mme*I type IIS restriction endonuclease (NEB, Pickering, Ontario, Canada). The digested 5′-terminal cDNA fragments were bound to streptavidin-coated magnetic beads (Dynal, Oslo, Norway). cDNA fragments that bound to the beads were directly ligated together in a reaction mixture containing T4 DNA ligase in a supplied buffer for 2.5 h at 16 °C. The ditags were amplified by PCR using the following primers: 5′ GGA TTT GCT GGT GCA GTA CA 3′ and 5′ CTG CTC GAA TGC AAG CTT CT 3′. The PCR products were analyzed by polyacrylamide gel electrophoresis (PAGE) and digested with *Eco*RI. The region of the gel containing the ditags was excised and the fragments were self-ligated to produce long concatamers that were then cloned into the *Eco*RI site of pZero 1.0 (Invitrogen). Colonies were screened by PCR using the M13 forward and reverse primers. PCR products containing inserts of more than 600 bp were sequenced with Big Dye terminator ver.3 and analyzed using a 3730 ABI automated DNA sequencer (Applied Biosystems, Foster City, CA, USA). All electrophoretograms were reanalyzed by visual inspection to check for ambiguous bases and to correct misreads. In this study, we obtained 19–20 bp tag information.

Association of the 5′SAGE tags with their corresponding genes

We attempted to align our 5′tags with the human genome (NCBI build 36, available from http://www.genome.ucsc.edu/) using the alignment program ALPS (http://www.alps.gi.k.u-tokyo.ac.jp/). Only tags that matched in sense orientation were considered in our analysis. The RefSeq database was searched for transcripts corresponding to the regions adjacent to the alignment location of each 5′tag.

RT-PCR

Total RNA was extracted using a ToTally RNA extraction kit (Ambion, Inc., Austin, TX, USA). Total RNA (500 ng) was reverse-transcribed in a 100-μl reaction solution containing 240 U of Moloney murine leukemia virus reverse transcriptase (Promega, Madison, WI, USA), 80 U of RNase inhibitor (Promega), 4.6 mM $MgCl_2$, 6.6 mM DTT, 1 mM dNTPs, and 2 mM random hexamer (Promega), at 42 °C for 1 h. PCR was performed in a 20-μl volume containing 0.5 U of AmpliTaq DNA polymerase (Applied Biosystems), 16.6 mM $(NH_4)_2SO_4$, 67 mM Tris–HCl, 6.7 mM $MgCl_2$, 10 mM 2-mercaptoethanol, 1 mM dNTPs, and 1.5 μM sense and antisense primers, using an ABI 9600 thermal cycler (Applied Biosystems). The amplification protocol included 28–30 cycles of 95 °C for 45 s, 58 °C for 1 min, and 72 °C for 1 min. Primer sequences are shown in Supplemental Table 2. RT-PCR was performed in triplicate for each sample-primer set. Each sample was normalized relative to *polymerase (RNA) II (DNA directed) polypeptide L (POLR2L)*. *POLR2L* is a housekeeping gene that showed relatively stable gene expression in various tissues [29]. The PCR products were semi-quantitatively analyzed with ImageJ software (http://rsb.info.nih.gov/ij/).

RTD-PCR

Intron-origin transcript expression was quantified using TaqMan Universal Master Mix (Applied Biosystems). The samples were amplified using an ABI PRISM 7900HT Sequence Detection System (Applied Biosystems). Using the standard curve methods, quantitative PCR was performed in duplicate for each sample-primer set. Each sample was normalized relative to *POLR2L*. The assay IDs used were Hs00185873_m1 for *ACOX2* and Hs00360764_m1 for *POLR2L*. The specific primers and probe sequence of intronic-*ACOX2-1* were 5′-TTCATAAAGTTGTGAGCA-GAGGAAA-3′ (forward), 5′-TGCACCACTTACTGAGCATCTACTC-3′ (reverse), and 5′-ACTTCTTACCTCAGAGCTG-3′ (probe).

Analysis of pathway network

MetaCore™ software (GeneGo Inc., St. Joseph, MI) was used to investigate the molecular pathway networks of non-B, non-C HCC, HBV-HCC and HCV-HCC. All genes up-regulated more than five-fold in all HCC libraries subjected to Enrichment analysis in GO process networks by default settings ($p<0.05$).

Statistical analysis

Kruskal–Wallis tests were used to compare the expression among normal liver, non-cancerous tissues, and HCC tissues. Mann–Whitney *U* tests were also used to evaluate the statistical significance of ACOX2

gene expression levels between two groups. All statistical analyses were performed using R (http://www.r-project.org/).

Acknowledgments

The authors would like to thank Mr. Shungo Deshimaru and Ms. Keiko Harukawa for technical assistance.

Appendix A. Supplementary data

Supplementary data associated with this article can be found, in the online version, at doi:10.1016/j.ygeno.2010.01.004.

References

[1] H.B. El-Serag, K.L. Rudolph, Hepatocellular carcinoma: epidemiology and molecular carcinogenesis, Gastroenterology 132 (2007) 2557–2576.
[2] Y. Yokoi, S. Suzuki, S. Baba, K. Inaba, H. Konno, S. Nakamura, Clinicopathological features of hepatocellular carcinomas (HCCs) arising in patients without chronic viral infection or alcohol abuse: a retrospective study of patients undergoing hepatic resection, J. Gastroenterol. 40 (2005) 274–282.
[3] R.N. Aravalli, C.J. Steer, E.N. Cressman, Molecular mechanisms of hepatocellular carcinoma, Hepatology 48 (2008) 2047–2063.
[4] D.J. Duggan, M. Bittner, Y. Chen, P. Meltzer, J.M. Trent, Expression profiling using cDNA microarrays, Nat. Genet. 21 (1999) 10–14.
[5] V.E. Velculescu, L. Zhang, B. Vogelstein, K.W. Kinzler, Serial analysis of gene expression, Science 270 (1995) 484–487.
[6] T. Yamashita, S. Hashimoto, S. Kaneko, S. Nagai, N. Toyoda, T. Suzuki, K. Kobayashi, K. Matsushima, Comprehensive gene expression profile of a normal human liver, Biochem. Biophys. Res. Commun. 269 (2000) 110–116.
[7] S. Hashimoto, S. Nagai, J. Sese, T. Suzuki, A. Obata, T. Sato, N. Toyoda, H.Y. Dong, M. Kurachi, T. Nagahata, K. Shizuno, S. Morishita, K. Matsushima, Gene expression profile in human leukocytes, Blood 101 (2003) 3509–3513.
[8] H. Okabe, S. Satoh, T. Kato, O. Kitahara, R. Yanagawa, Y. Yamaoka, T. Tsunoda, Y. Furukawa, Y. Nakamura, Genome-wide analysis of gene expression in human hepatocellular carcinomas using cDNA microarray: identification of genes involved in viral carcinogenesis and tumor progression, Cancer. Res. 61 (2001) 2129–2137.
[9] Y. Shirota, S. Kaneko, M. Honda, H.F. Kawai, K. Kobayashi, Identification of differentially expressed genes in hepatocellular carcinoma with cDNA microarrays, Hepatology 33 (2001) 832–840.
[10] T. Yamashita, M. Honda, S. Kaneko, Application of serial analysis of gene expression in cancer research, Curr. Pharm. Biotechnol. 9 (2008) 375–382.
[11] Y. Suzuki, H. Taira, T. Tsunoda, J. Mizushima-Sugano, J. Sese, H. Hata, T. Ota, T. Isogai, T. Tanaka, S. Morishita, K. Okubo, Y. Sakaki, Y. Nakamura, A. Suyama, S. Sugano, Diverse transcriptional initiation revealed by fine, large-scale mapping of mRNA start sites, EMBO Rep. 2 (2001) 388–393.
[12] K. Kimura, A. Wakamatsu, Y. Suzuki, T. Ota, T. Nishikawa, R. Yamashita, J. Yamamoto, M. Sekine, K. Tsuritani, H. Wakaguri, S. Ishii, T. Sugiyama, K. Saito, Y. Isono, R. Irie, N. Kushida, T. Yoneyama, R. Otsuka, K. Kanda, T. Yokoi, H. Kondo, M. Wagatsuma, K. Murakawa, S. Ishida, T. Ishibashi, A. Takahashi-Fujii, T. Tanase, K. Nagai, H. Kikuchi, K. Nakai, T. Isogai, S. Sugano, Diversification of transcriptional modulation: large-scale identification and characterization of putative alternative promoters of human genes, Genome. Res. 16 (2006) 55–65.
[13] T. Shiraki, S. Kondo, S. Katayama, K. Waki, T. Kasukawa, H. Kawaji, R. Kodzius, A. Watahiki, M. Nakamura, T. Arakawa, S. Fukuda, D. Sasaki, A. Podhajska, M. Harbers, J. Kawai, P. Carninci, Y. Hayashizaki, Cap analysis gene expression for high-throughput analysis of transcriptional starting point and identification of promoter usage, Proc. Natl. Acad. Sci. U. S. A. 100 (2003) 15776–15781.
[14] S. Hashimoto, Y. Suzuki, Y. Kasai, K. Morohoshi, T. Yamada, J. Sese, S. Morishita, S. Sugano, K. Matsushima, 5′-end SAGE for the analysis of transcriptional start sites, Nat. Biotechnol. 22 (2004) 1146–1149.
[15] T. Yamashita, S. Kaneko, S. Hashimoto, T. Sato, S. Nagai, N. Toyoda, T. Suzuki, K. Kobayashi, K. Matsushima, Serial analysis of gene expression in chronic hepatitis C and hepatocellular carcinoma, Biochem. Biophys. Res. Commun. 282 (2001) 647–654.
[16] T. Yamashita, M. Honda, H. Takatori, R. Nishino, H. Minato, H. Takamura, T. Ohta, S. Kaneko, Activation of lipogenic pathway correlates with cell proliferation and poor prognosis in hepatocellular carcinoma, J. Hepatol. 50 (2009) 100–110.
[17] J.S. Mattick, Introns: evolution and function, Curr. Opin. Genet. Dev. 4 (1994) 823–831.
[18] J.S. Mattick, I.V. Makunin, Non-coding RNA, Hum. Mol. Genet. 15 (Spec No 1) (2006) R17–29.
[19] R. Louro, A.S. Smirnova, S. Verjovski-Almeida, Long intronic noncoding RNA transcription: expression noise or expression choice? Genomics 93 (2009) 291–298.
[20] S. Yu, S. Rao, J.K. Reddy, Peroxisome proliferator-activated receptors, fatty acid oxidation, steatohepatitis and hepatocarcinogenesis, Curr. Mol. Med. 3 (2003) 561–572.
[21] N. Kondoh, T. Wakatsuki, A. Ryo, A. Hada, T. Aihara, S. Horiuchi, N. Goseki, O. Matsubara, K. Takenaka, M. Shichita, K. Tanaka, M. Shuda, M. Yamamoto, Identification and characterization of genes associated with human hepatocellular carcinogenesis, Cancer. Res. 59 (1999) 4990–4996.
[22] Y. Kobayashi, T. Higashi, K. Nouso, H. Nakatsukasa, M. Ishizaki, T. Kaneyoshi, N. Toshikuni, K. Kariyama, E. Nakayama, T. Tsuji, Expression of MAGE, GAGE and BAGE genes in human liver diseases: utility as molecular markers for hepatocellular carcinoma, J. Hepatol. 32 (2000) 612–617.
[23] A.H. Minn, M. Kayton, D. Lorang, S.C. Hoffmann, D.M. Harlan, S.K. Libutti, A. Shalev, Insulinomas and expression of an insulin splice variant, Lancet 363 (2004) 363–367.
[24] H. Stier, H.D. Fahimi, P.P. Van Veldhoven, G.P. Mannaerts, A. Volkl, E. Baumgart, Maturation of peroxisomes in differentiating human hepatoblastoma cells (HepG2): possible involvement of the peroxisome proliferator-activated receptor alpha (PPAR alpha), Differentiation 64 (1998) 55–66.
[25] S. Zha, S. Ferdinandusse, J.L. Hicks, S. Denis, T.A. Dunn, R.J. Wanders, J. Luo, A.M. De Marzo, W.B. Isaacs, Peroxisomal branched chain fatty acid beta-oxidation pathway is upregulated in prostate cancer, Prostate 63 (2005) 316–323.
[26] K. Tokuoka, Y. Nakajima, K. Hirotsu, I. Miyahara, Y. Nishina, K. Shiga, H. Tamaoki, C. Setoyama, H. Tojo, R. Miura, Three-dimensional structure of rat-liver acyl-CoA oxidase in complex with a fatty acid: insights into substrate-recognition and reactivity toward molecular oxygen, J. Biochem. 139 (2006) 789–795.
[27] K. Meyer, Y. Jia, W.Q. Cao, P. Kashireddy, M.S. Rao, Expression of peroxisome proliferator-activated receptor alpha, and PPARalpha regulated genes in spontaneously developed hepatocellular carcinomas in fatty acyl-CoA oxidase null mice, Int. J. Oncol. 21 (2002) 1175–1180.
[28] N. Tanaka, K. Moriya, K. Kiyosawa, K. Koike, F.J. Gonzalez, T. Aoyama, PPARalpha activation is essential for HCV core protein-induced hepatic steatosis and hepatocellular carcinoma in mice, J. Clin. Invest. 118 (2008) 683–694.
[29] C. Rubie, K. Kempf, J. Hans, T. Su, B. Tilton, T. Georg, B. Brittner, B. Ludwig, M. Schilling, Housekeeping gene variability in normal and cancerous colorectal, pancreatic, esophageal, gastric and hepatic tissues, Mol. Cell. Probes. 19 (2005) 101–109.

Liver INTERNATIONAL
OFFICIAL JOURNAL OF THE INTERNATIONAL ASSOCIATION FOR THE STUDY OF THE LIVER

Liver International ISSN 1478-3223

CLINICAL STUDIES

dUTP pyrophosphatase expression correlates with a poor prognosis in hepatocellular carcinoma

Hajime Takatori[1], Taro Yamashita[1], Masao Honda[1], Ryuhei Nishino[1], Kuniaki Arai[1], Tatsuya Yamashita[1], Hiroyuki Takamura[2], Tetsuo Ohta[2], Yoh Zen[3] and Shuichi Kaneko[1]

1 Department of Gastroenterology, Kanazawa University Graduate School of Medical Science, Ishikawa, Japan
2 Department of Gastroenterologic Surgery, Kanazawa University Graduate School of Medical Science, Ishikawa, Japan
3 Pathology Section, Kanazawa University Hospital, Ishikawa, Japan

Keywords
dUTP pyrophosphatase – hepatocellular carcinoma – prognosis – serial analysis of gene expression

Abbreviations
5-FU, 5-fluorouracil; dUTPase, dUTP pyrophosphatase; HCC, hepatocellular carcinoma; IHC, immunohistochemistry; qRT-PCR, quantitative reverse transcription-polymerase chain reaction; SAGE, serial analysis of gene expression.

Correspondence
Masao Honda, MD, Department of Gastroenterology, Kanazawa University Graduate School of Medical Science, 13-1 Takara-Machi, Kanazawa, Ishikawa 920-8641, Japan
Tel: +81 76 265 2233
Fax: +81 76 234 4250
e-mail: mhonda@m-kanazawa.jp

Received 13 August 2009
Accepted 26 October 2009

DOI:10.1111/j.1478-3231.2009.02177.x

Abstract

Background: Hepatocellular carcinoma (HCC) is a malignancy with a poor prognosis, partly owing to the lack of biomarkers that support its classification in line with its malignant nature. To discover a novel molecular marker that is related to the efficacy of treatment for HCC and its biological nature, we performed serial analysis of gene expression (SAGE) in HCC, normal liver and cirrhotic liver tissues. *Methods:* Gene expression profiles of HCC tissues and non-cancerous liver tissues were obtained by SAGE. Suppression of the target gene by RNA interference was used to evaluate its role in HCC *in vitro*. The relation of the identified marker and prognosis was statistically examined in surgically resected HCC patients. *Results:* We identified significant over-expression of *DUT*, which encodes dUTP pyrophosphatase (dUTPase), in HCC tissue, and this was confirmed in about two-thirds of the HCC samples by reverse-transcription polymerase chain reaction ($n = 20$). Suppression of dUTPase expression using short interfering RNAs inhibited cell proliferation and sensitized HuH7 cells to 5-fluorouracil treatment. Nuclear dUTPase expression was observed in 36.6% of surgically resected HCC samples ($n = 82$) evaluated by immunohistochemistry, and its expression was significantly correlated with the histological grades ($P = 0.0099$). Notably, nuclear dUTPase expression correlated with a poor prognosis with statistical significance (HR, 2.47; 95% CI, 1.08–5.66; $P = 0.032$). *Conclusion:* Taken together, these results suggest that nuclear dUTPase may be a good biomarker for predicting prognosis in HCC patients after surgical resection. Development of novel dUTPase inhibitors may facilitate the eradication of HCC.

Hepatocellular carcinoma (HCC) is the fifth most common malignancy and the third leading cause of cancer-related death worldwide (1). Several risk factors are responsible for HCC development, including alcoholism, aflatoxin and genetic diseases such as haemochromatosis and α-1 antitrypsin deficiency; however, the major risk factor is chronic hepatitis owing to hepatitis B virus (HBV) or hepatitis C virus (HCV) infection (2–4). Several treatment options are currently available for HCC management, which include liver transplantation, surgical resection, percutaneous ethanol injection, radiofrequency ablation, transcatheter arterial chemoembolization and systemic or local chemotherapy, and optimal treatment is determined based on tumour stage and liver function (5, 6). However, more than 80% of HCC cases develop advanced HCC after initial treatment (7).

Various chemotherapeutic drugs have been investigated for their antitumour activity in advanced HCC. For example, 5-fluorouracil (5-FU), a thymidylate synthase inhibitor, was the first reported drug studied for the treatment of advanced HCC; however, a median survival rate of 3–5 months has discouraged the further use of 5-FU as a single chemotherapeutic agent (8, 9). Interferon-α (IFN-α) has been reported to have antitumour activity against advanced HCC, and recent reports have suggested the efficacy of a combination of 5-FU/IFN-α for advanced HCC treatment (10–12), although convincing evidence for improved survival rate remains lacking. A recent study has indicated that 16% of advanced HCC patients responded positively to 5-FU/IFN-α treatment with clear and significant survival benefits compared with stable or progressive disease